Cretaceous deformation, Chegitun River area, Chukotka Peninsula, Russia: Implications for the tectonic evolution of the Bering Strait region

Jaime Toro

Department of Geology and Geography, West Virginia University, Morgantown, West Virginia, USA

Jeffrey M. Amato

Department of Geological Sciences, New Mexico State University, Las Cruces, New Mexico, USA

Boris Natal'in

Istanbul Technical University, Istanbul, Turkey

Received 9 October 2001; revised 1 August 2002; accepted 19 September 2002; published 30 May 2003.

[1] The Koolen metamorphic dome of Chukotka Peninsula has been interpreted as a mid-Cretaceous extensional core complex. On the NW flank of the dome, three lithotectonic units are exposed: (1) High-Grade unit, composed of sillimanite-grade rocks; (2) Tanatap unit, composed of polydeformed greenschist-grade phyllites and marbles; (3) Chegitun unit composed of unmetamorphosed early Paleozoic limestones. Four Early Cretaceous to Tertiary deformational events are documented. D_1 is attributed to the collisional closure of the South Anyui suture. The $^{40}Ar/^{39}Ar$ ages from the Tanatap unit constrain this event at 117–124 Ma. Relict kyanite-bearing assemblages in the High-Grade unit probably formed during this event under moderately high pressure conditions. D_2 is related to extensional deformation in the Koolen dome. In the High-Grade unit, sillimanite-grade metamorphism was followed by rapid cooling and exhumation at 109–104 Ma. In the Tanatap unit, early fabrics underwent isoclinal folding, and a new cleavage (S_{2t}) was developed. The kinematics of the High-Grade unit indicates ductile deformation by top-to-the-south shear, as is the case in the dome core. This suggests that the Koolen dome is a unidirectional core complex formed by south directed extension. We believe collapse of overthickened crust caused extension in the Koolen dome. The crust was thickened during Early Cretaceous collision and during subsequent oroclinal bending of the structures in the Bering Strait region. The youngest structures in the Chegitun Valley are NW striking normal faults kinematically linked to NE striking right-lateral strike-slip faults. They are probably the continuation of structures found offshore in the Hope Basin. *INDEX TERMS:* 8109 Tectonophysics: Continental tectonics—extensional (0905); 8025 Structural Geology: Mesoscopic fabrics; 1035 Geochemistry: Geochronology; 8005 Structural Geology: Folds and folding; *KEYWORDS:* Koolen Dome, extension, Arctic, thermochronology, core complex. **Citation:** Toro, J., J. M. Amato, and B. Natal'in, Cretaceous deformation, Chegitun River area, Chukotka Peninsula, Russia: Implications for the tectonic evolution of the Bering Strait region, *Tectonics*, *22*(3), 1021, doi:10.1029/2001TC001333, 2003.

Copyright 2003 by the American Geophysical Union.
0278-7407/03/2001TC001333

1. Introduction

[2] High-grade gneiss domes of Cretaceous age have been mapped in the Bering Strait region (Figure 1) both on the Chukotka Peninsula of northeastern Russia [*Natal'in*, 1979; *Parfenov and Natal'in*, 1979; *Bering Strait Geologic Field Party* (BSGFP), 1997] and the Seward Peninsula of Alaska [*Armstrong et al.*, 1986; *Dusel-Bacon et al.*, 1989; *Amato et al.*, 1994]. These metamorphic culminations are similar to the deepest exposed levels of metamorphic core complexes and are thought to have formed during an important episode of magmatism and thinning of the crust in the Bering Strait region [*Miller and Hudson*, 1991; *Dumitru et al.*, 1995; *BSGFP*, 1997; *Klemperer et al.*, 2002]. The core complexes of the Bering Strait region formed in close proximity to a subduction zone. In this respect their setting is similar to the Neogene extensional complexes of the Aegean. However, this similarity is superficial. Important differences in the crustal structure of the two regions prior to the onset of extension, the overall plate interactions, and their subsequent evolution lead us to believe that different mechanisms for extension were in play.

[3] In the classic Cordilleran core complexes the structural relationship between high-grade rocks in the deeper structural levels and the brittlely deformed rocks that lie above the detachment fault has been well established. However, in the gneiss domes of the Bering Strait upper plate rocks with a clear history of brittle extensional faulting have not been documented. We expected to find clear upper plate/lower plate relationships in the Chegitun River valley

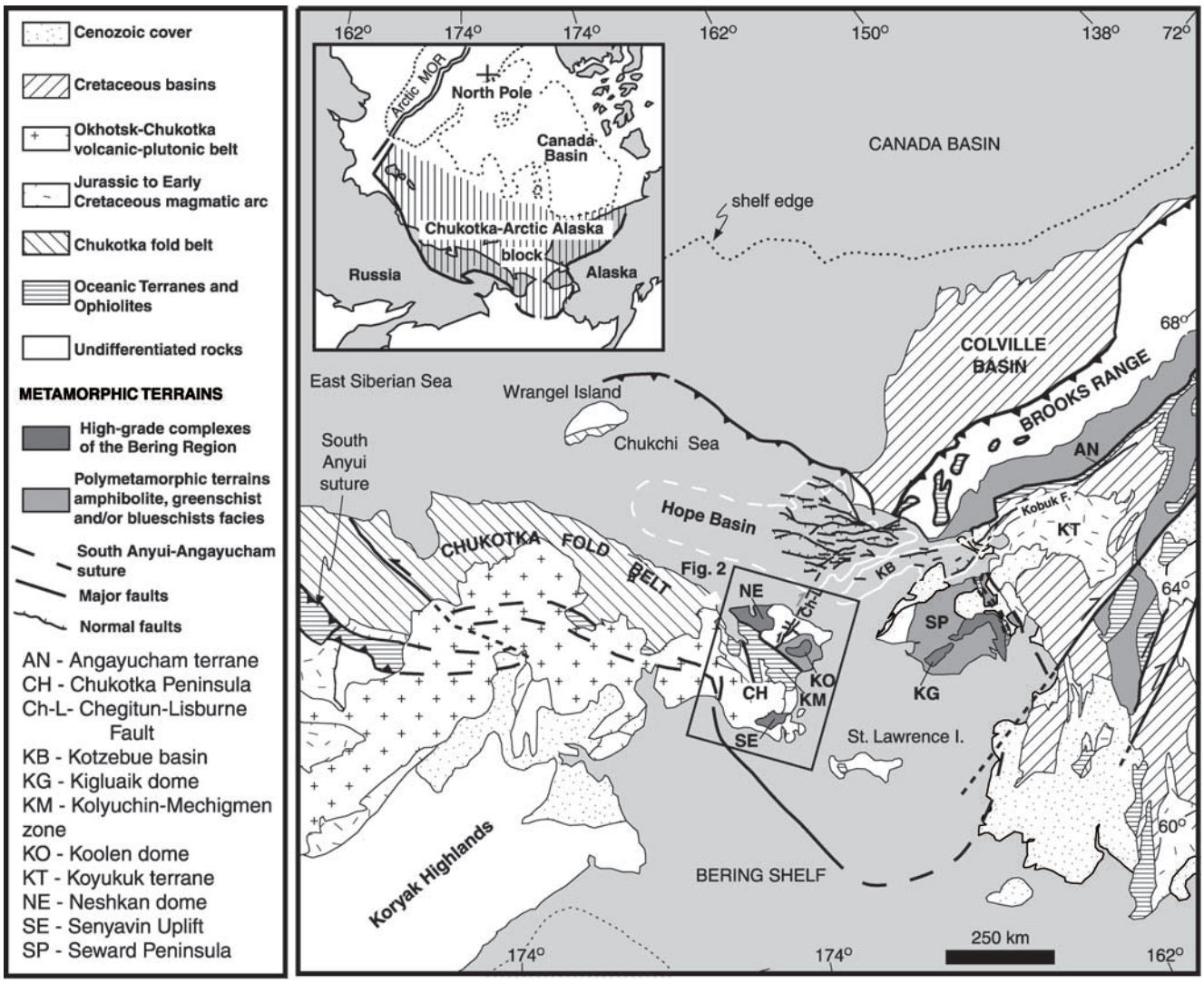

Figure 1. Location map showing northeastern Russia and northwestern Alaska [after *Natal'in*, 1984; *Tolson*, 1987; *Haimila et al.*, 1990; *Moore et al.*, 1994a, 1994b; *Plafker and Berg*, 1994; *Natal'in*, 1999]. The inset map shows the Chukotka–Arctic Alaska block.

of northern Chukotka Peninsula, where a weakly metamorphosed lower Paleozoic carbonate and Devonian to Lower Carboniferous siliclastic rocks are in fault contact with rocks of the Koolen metamorphic dome (Figure 2). However, the structural relationships observed in the Chegitun Valley are complex, and the contacts between supracrustal and deep-level rocks are overprinted by postextensional strike-slip faulting.

[4] In this paper we describe structural and thermochronologic data from the northwest margin of the Koolen dome and their implications for the formation of high-grade gneiss domes in the Bering Strait region, as well as for the Mesozoic tectonic history of the Chukotka–Arctic Alaska block. In a previous paper we discussed the regional stratigraphic/tectonic implications of the Paleozoic units exposed in the Chegitun Valley and their correlation with similar rocks in northern Alaska [*Natal'in et al.*, 1999]. Details of the latest Cretaceous-Tertiary evolution of northern Chukotka Peninsula and surrounding regions are given by *Natal'in* [1999].

2. Geologic Setting

[5] Correlation of tectonostratigraphic units across the Bering Strait suggests that the Chukotka Peninsula of northeastern Russia (Figure 1) is part of a continental block that consists of the Brooks Range, Colville Basin, Beaufort Shelf, and Seward Peninsula on the North American side and part of northeastern Russia including most of the immense East Siberian Shelf [*Parfenov and Natal'in*, 1977, 1985; *Fujita and Newberry*, 1982; *Zonenshain et al.*, 1990]. The Mesozoic evolution of this small continent, known as the Chukotka–Arctic Alaska block (Figure 1),

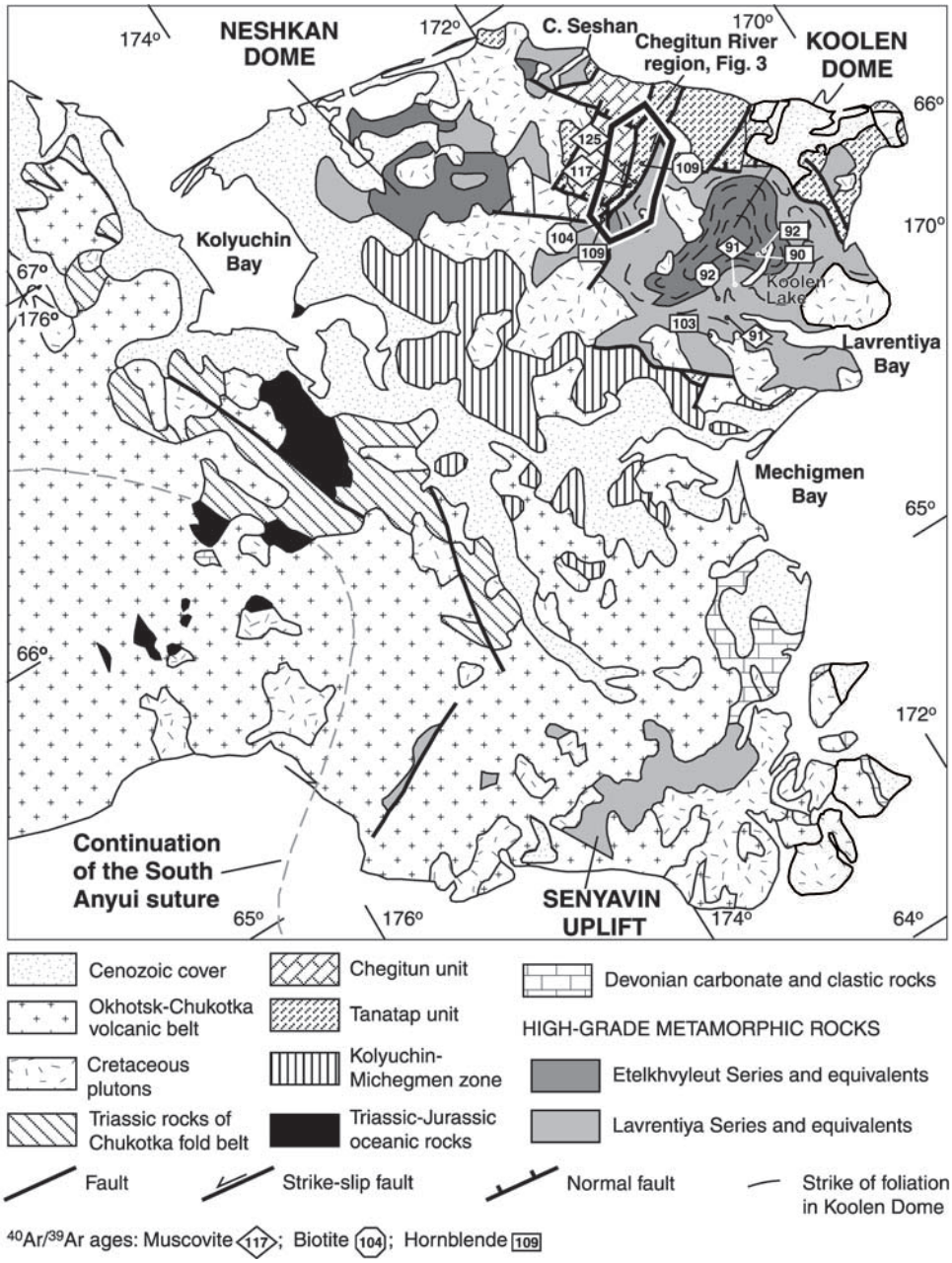

Figure 2. Geological map of Chukotka Peninsula modified from *Gorodinsky* [1980]. Representative $^{40}Ar/^{39}Ar$ ages from the Koolen dome and the Senyavin uplift are shown (from *Calvert* [1999], *Akinin and Calvert* [2002], and our data).

has been determined by tectonic events linked to the opening of the Canada basin to the north [*Natal'in*, 1984; *Grantz et al.*, 1990] and collisional deformation along its southern boundary. Many of the details of the evolution of the Chukotka-Arctic-Alaska block remain controversial [e.g., *Lawver and Scotese*, 1990].

[6] The southern boundary of the Chukotka–Arctic Alaska block is marked by belts of ophiolites and oceanic rocks (Figure 1): the South Anyui suture of Chukotka [*Natal'in*, 1984; *Sokolov et al.*, 2002; *Zonenshain et al.*, 1990] and the Angayucham terrane of northern Alaska [*Moore et al.*, 1994a, 1994b]. Workers in the Brooks Range attribute the emplacement of the Angayucham terrane to closure of a marginal ocean basin and collision of the Koyukuk arc against the Chukotka-Alaska margin [*Patton and Box*, 1989]. In eastern Chukotka the South Anyui suture was formed because of collision with early Mesozoic arcs and continental blocks that are exposed in the Koryak Highlands (Figure 1) [*Natal'in*, 1984]. The Kolyuchin-Mechigmen zone, located directly south of the Koolen dome (Figures 1 and 2), contains Jurassic gabbro and chert probably correlative with rocks of the South

Anyui–Angayucham suture zone. It is unclear whether the Kolyuchin-Mechigmen zone is a klippe similar to the Brooks Range ophiolites or a strike-slip duplication of part of the suture. In Alaska, intense contractional deformation within the Chukotka–Arctic Alaska block occurred mostly during Neocomian time but continued until the end of the Albian [*Moore et al.*, 1994a, 1994b]. An extensive high-pressure/low-temperature metamorphic belt related to this collision occurs immediately to the north and structurally below the Angayucham terrane and has been traced from the eastern Brooks Range west onto the Seward Peninsula [*Patrick and Evans*, 1989]. To the north of the high-pressure/low-temperature metamorphic rocks a classic supracrustal fold-and-thrust belt makes up the bulk of the Brooks Range and extends into the Colville foreland basin to the north [e.g., *Moore et al.*, 1994a, 1994b]. The equivalent of this fold-and-thrust belt on the western side of the Bering Strait is the Chukotka fold belt (Figure 1), which consists of thick Triassic and Early Jurassic continental margin clastic deposits deformed along the South Anyui suture [*Natal'in*, 1984; *Parfenov and Natal'in*, 1985]. Given the similar geologic history along the length of the Chukotka–Arctic Alaska block, it is likely that during Early Cretaceous time this region was a continuous contractional orogenic belt. However, in Chukotka this collisional belt was relatively short-lived. Aptian-Albian gently folded sedimentary and volcanic rocks overlap the Neocomian South Anyui suture zone indicating that shortening lasted only between the Hauterivian and Aptian. The apparent absence of foreland basins in Chukotka suggests that shortening was not as strong as in northern Alaska. Studies in the Seward Peninsula show that the collision-related metamorphic fabrics were overprinted in the mid-Cretaceous by high-grade metamorphic domes associated with granitic magmatism [*Patrick and Evans*, 1989; *Miller et al.*, 1992; *Amato et al.*, 1994]. Isotopic dating of the metamorphic fabrics in the Kigluaik gneiss dome of Seward Peninsula have revealed that large-magnitude extension and wholesale thinning of the crust took place between 105 and 91 Ma [*Amato et al.*, 1994; *Amato and Wright*, 1998]. Crustal thickness in the low-lying Bering Strait region is a relatively thin 32 km [*Klemperer et al.*, 2002].

[7] Three gneiss domes similar to the Kigluaik dome are exposed on the Chukotka Peninsula (Figure 2): the Senyavin uplift in the south and the Koolen and Neshkan domes in the north [*Shuldiner and Nedomolkin*, 1976; *Natal'in*, 1979]. All three are associated with mid-Cretaceous granitic plutons. These plutons are part of the immense subduction-related magmatic belt that existed along the Paleo-Pacific margin during the Middle and Late Cretaceous [*Parfenov and Natal'in*, 1977; *Plafker and Berg*, 1994; *Rubin et al.*, 1995; *Amato and Wright*, 1998]. The southern part of Chukotka Peninsula is covered by volcanic deposits of the Middle and Late Cretaceous Okhotsk-Chukotka volcanic belt, which are probably the extrusive equivalents of the plutons exposed farther north (Figure 2).

[8] The study area is located on the northwest flank of the Koolen dome. Second-sillimanite-grade Etelkhvyleut Series gneisses with abundant evidence for partial melting occur in the core of the dome [*Nedomolkin*, 1969, 1977; *Shuldiner and Nedomolkin*, 1976; *BSGFP*, 1997]. In the Koolen Lake region, where the deepest structural levels are exposed (Figure 2), peak metamorphic conditions are 600–800 MPa and >700°C [*Akinin and Calvert*, 2002]. The flanks of the dome are somewhat lower grade and include pelitic schists, paragneisses, and marbles with sillimanite + muscovite-bearing assemblages. These rocks are mapped as the Lavrentiya Series [*Nedomolkin*, 1977]. U-Pb geochronology of monazite from metamorphic rocks and cross-cutting aplite dikes brackets high-grade metamorphism at 104–94 Ma [*BSGFP*, 1997], which is essentially identical to the timing of formation of the Kigluaik dome of Seward Peninsula. However, orthogneisses with both late Precambrian and Devonian zircon ages occur within the Lavrentiya and the Etelkhvyleut Series [*Natal'in et al.*, 1999], and Rb-Sr whole rock isochron ages as old as 1990 ± 55 Ma [*Zhulanova*, 1990] indicate that the protoliths of the Koolen dome are older and may have undergone a complex and protracted pre-Cretaceous magmatic and metamorphic history.

[9] Foliation in the Koolen area gneisses dips gently to the south, and mineral lineations generally trend south and southeast and show top-to-the-south and top-to-southeast sense of shear [*BSGFP*, 1997]. Stretching lineations in the higher structural levels of the Kigluaik gneiss dome trend to the north, but, in contrast to the Koolen dome, these lineations reveal top-to-north sense of shear [*Patrick*, 1988; *Miller et al.*, 1992; *Hannula et al.*, 1995]. In spite of this difference the similarity in lithologies of the rocks involved, the synchronous timing of deformation and magmatism, and the overall structure of both regions suggest that the mid-Cretaceous extensional episode was regional in nature [*Miller and Hudson*, 1991]. As is the case for the Kigluaik dome, a detachment fault has not been identified in Chukotka though thick zones of mylonite parallel to foliation were mapped within the high-grade rocks [*BSGFP*, 1997]. We interpret the absence of clear lower/upper plate relationships as a result of deep erosion and overprinting by later faulting.

3. Geology of the Chegitun Valley

[10] The Chegitun River Valley is located along the northwestern margin of the Koolen dome (Figure 2). Recent incision by the Chegitun River and its tributaries has produced nearly continuous outcrops along the river banks. We were able to carry out a detailed kinematic study of the area, but because the outcrop belt tends to parallel the main structural grain, few exposures of the boundaries between the main lithotectonic units were found. The area has been divided into three fault-bounded northeast striking lithotectonic units (Figure 3) [*Natal'in et al.*, 1999]. From southeast to northwest these are (1) the High-Grade unit, which consists of sillimanite- and higher-grade rocks intruded by Cretaceous granitic plutons; (2) the Tanatap unit, which consists of polydeformed low-grade-greenschist calcareous

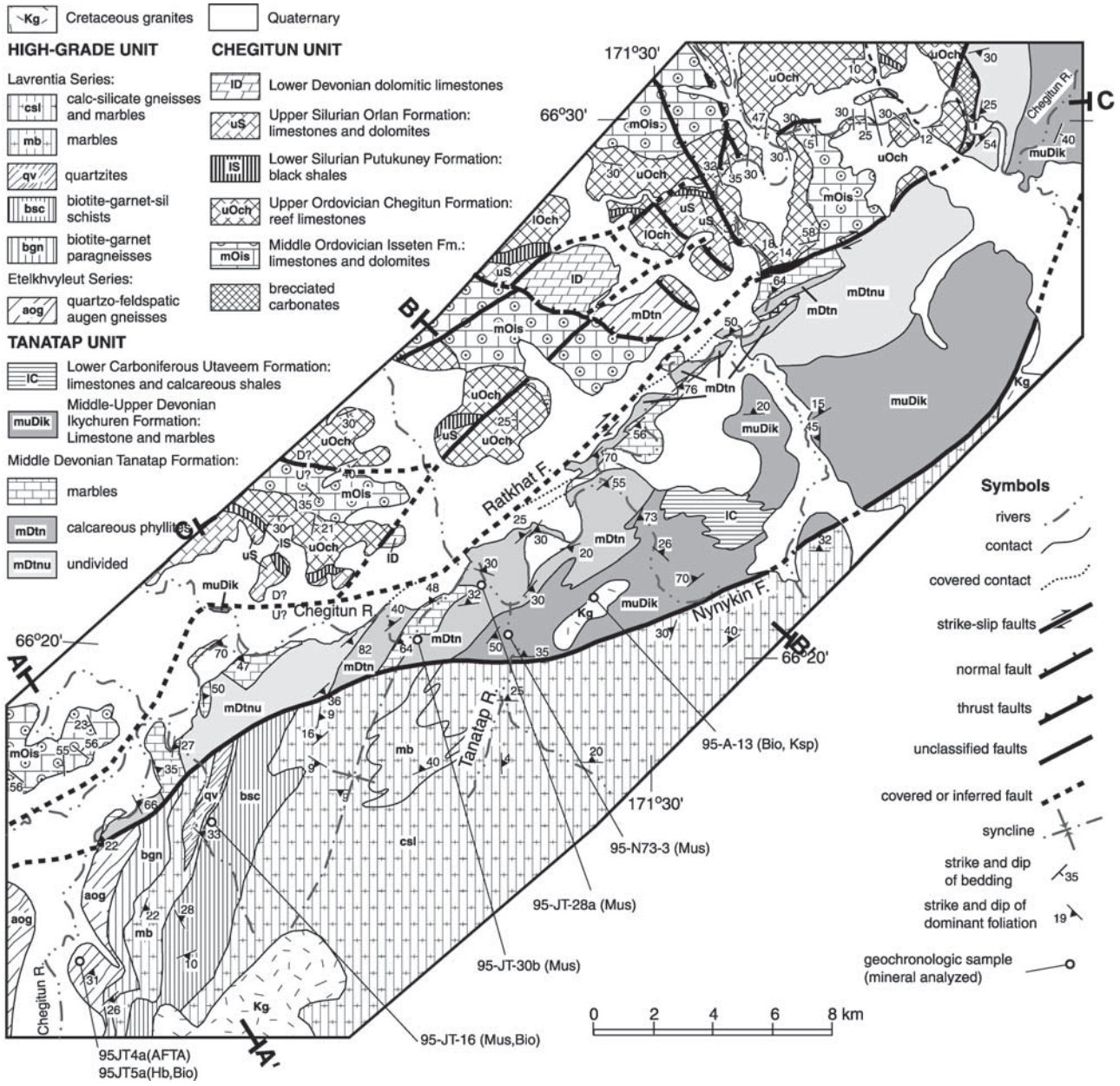

Figure 3. Geological map of the Chegitun River Valley. Location of the map area is shown on Figure 2.

phyllites, marbles, and metatuffs with probable Devonian protolith ages; and (3) the Chegitun unit which consists of virtually unmetamorphosed Ordovician to Lower Devonian platform carbonates. These three lithotectonic units are separated by two northeast trending, steeply dipping faults that postdate ductile deformation and metamorphism of the area and that obscure the primary relationship between the units. These are the Ratkhat and Nynykin faults, which on the basis of kinematic data we interpret as right-lateral strike-slip faults [*Natal'in et al.*, 1999]. In discussing the metamorphic fabrics of the Chegitun region we use S_{1h}, L_{1h}, and F_{1h} to designate the structural features (foliation, lineations, and fold axes) related to the earliest deformational event (D_{1h}) recognized in the High-Grade unit, whereas S_{1t}, L_{1t}, F_{1t}, etc., designate the structural features of the Tanatap unit.

3.1. Deformation and Metamorphism in the High-Grade Unit

[11] The High-Grade unit (Figure 3) consists of banded granitic augen gneisses interlayered with 1- to 30-m-thick layers of marble and thin bands of amphibolitic metagabbros. These are overlain by a dominantly metasedimentary section composed of calc-silicates, marbles, and minor pelitic schists (Figure 4). The deeper, dominantly metaigneous section is part of the Etelkhvyleut Series of the Koolen dome, whereas the structurally higher, lower-grade

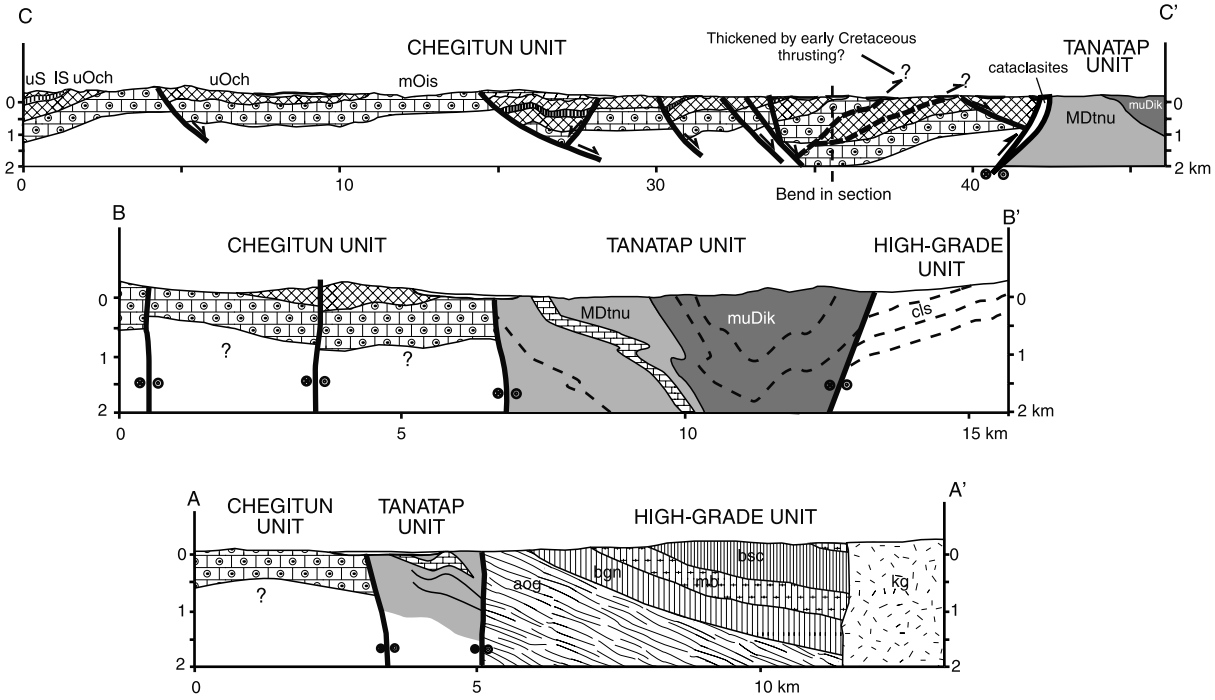

Figure 4. Structural cross sections of the Chegitun River Valley. The cross section C-C′ is modified after *Natal'in* [1999]. Location of the sections is shown on Figure 3.

and dominantly metasedimentary section is part of the Lavrentiya Series [*Nedomolkin*, 1969, 1977; *Shuldiner and Nedomolkin*, 1976]. In the Chegitun Valley the metamorphic grade of the Etelkhvyleut Series is somewhat lower with no evidence of the partial melting that is conspicuous in the core of the dome. In addition, interlayered metapelitic rocks are sillimanite-muscovite-bearing instead of second-sillimanite-grade as in the core of the dome. Recent U-Pb geochronology has shown that the protoliths of Etelkhvyleut Series include late Precambrian and Devonian orthogneisses [*Natal'in et al.*, 1999], as well as mid-Cretaceous orthogneisses [*BSGFP*, 1997]. Metapelitic rocks within the High-Grade unit display two main metamorphic assemblages: (1) an older assemblage characterized by biotite, garnet, white mica, and kyanite, which was previously recognized by *Shuldiner and Nedomolkin* [1976], and (2) a younger assemblage, in which garnet is replaced by cordierite (Figure 5a), sillimanite grows in the strain shadows of kyanite porphyroblasts (Figure 5b), and there is wholesale replacement of kyanite by sillimanite. In general, the rocks are very fresh, although locally there is minor chlorite growth in fractures that cut the garnets.

[12] Although quantitative thermobarometric studies have not been carried out on the Chegitun Valley samples, the assemblages present and their relationships allow us to approximate the pressure-temperature (P-T) history of the rocks (Figure 6). The older, kyanite-bearing assemblage represents moderate to high pressure at temperatures below minimum melting conditions, whereas the younger, cordierite- and sillimanite-bearing assemblage attests to a drop in pressure and, perhaps, a moderate increase in temperature. This second assemblage is best developed in the southern part of map area (Figure 3). The textures indicate that the second assemblage is synkinematic with high-strain ductile deformation and with the development of the dominant metamorphic foliation in the High-Grade unit.

[13] In the sillimanite-grade Etelkhvyleut Series the S_{2h} foliation is dominant, although relicts of an earlier mineral assemblage are locally preserved (Figure 5). Mineral stretching lineations (L_{2h}) associated with the dominant fabric are well developed in most lithologies in the High-Grade unit and consistently trend N-S (Figure 7a). Kinematic indicators, such as asymmetric strain shadows around porphyroblasts and mica fish, indicate that sense of motion was top to the south during the D_{2h} event (Figure 8a). This sense of shear is consistent with that observed in Lavrentiya Series rocks near the core of the Koolen dome [*BSGFP*, 1997].

[14] Mineral assemblages in the calc-silicate gneisses and schists of the Lavrentiya Series (unit csl, Figure 3) indicate a metamorphic grade lower than in the Etelkhvyleut Series. In contrast to rocks farther south, sillimanite is absent in pelitic lithologies. *Shuldiner and Nedomolkin* [1976] report finding kyanite-bearing assemblages in the uppermost structural level of our calc-silicate unit. We interpret them as the relict assemblages indicating that D_1 metamorphism and deformation was regional. Besides, these rocks preserve two foliations, which we label as S_{2h} and S_{3h}. S_{2h} is represented by coarse biotite and muscovite in pelitic lithologies. The dominant foliation (S_{2h}) is usually gently dipping. In the southwestern portion of our map area it dips gently to the southeast, while over the rest of our map the dominant dip is to the northwest (Figures 3 and 7a). The northwest dipping foliation defines the domal shape

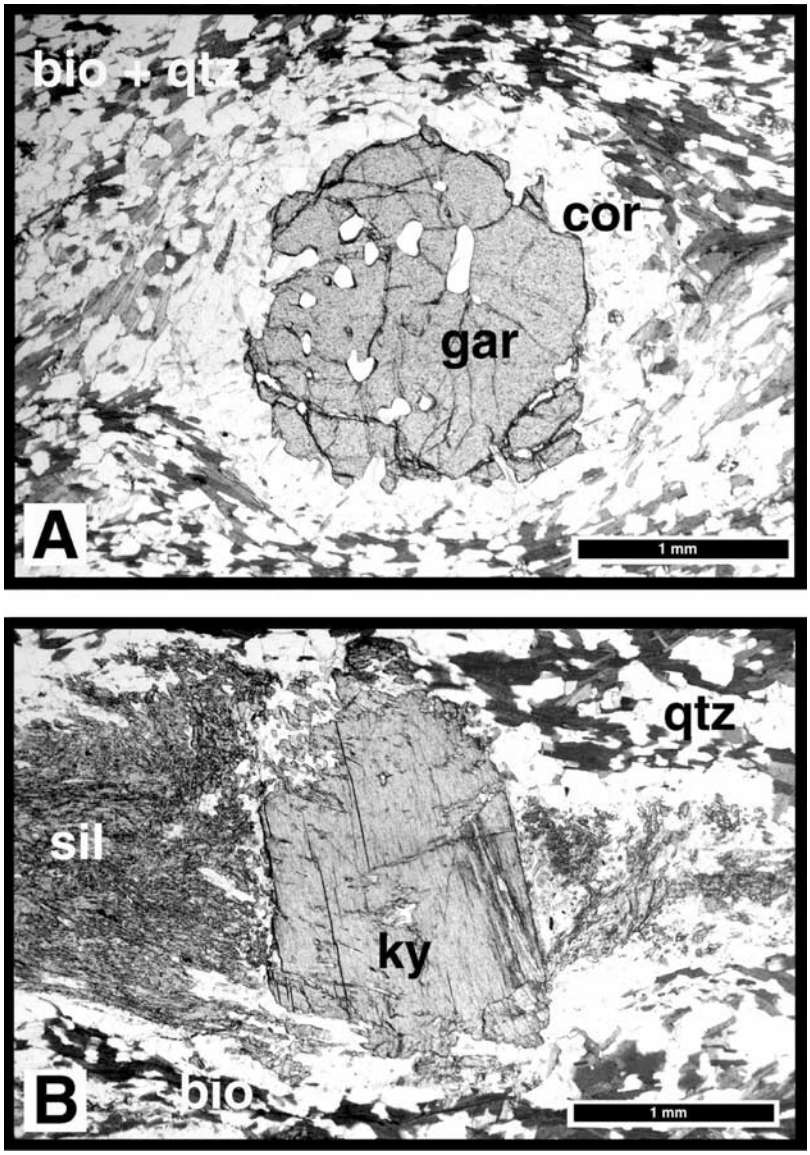

Figure 5. Photomicrographs of biotite-garnet-sillimanite schist (bsc) of the Lavrentiya Series in the High-Grade unit. (a) Garnet of the early metamorphic assemblage replaced by a cordierite rim. (b) Sillimanite, syntectonic with the dominant foliation (S_{2h}), developed in the strain shadow of a kyanite porphyroblast.

of the Koolen metamorphic complex, although the variations observed across the map show that the High-Grade unit is folded by broad folds with north trending axes (Figure 7a). These folds have also been recognized in the core of the dome [*BSGFP*, 1997] and suggest late stage E-W shortening across the dome.

[15] Recumbent isoclinal folds (F_{3h}) deform the S_{2h} foliation in a zone 1 km wide of the upper Tanatap Valley. These folds are northeast trending and southeast verging and varying in scale from one to tens of meters. The S_{3h} foliation is axial-planar to these folds and is defined by new fine-grained mica and biotite growth as well as by pressure-solution seams. The S_{3h} foliation fades away to the east. In the Koolen Lake region we observed folds whose geometry, orientation, and vergence are similar to the F_{3h} folds of the Tanatap Valley, but no axial-planar foliation was noted there.

[16] In summary, we found evidence for two major metamorphic events within the High-Grade unit. The first event is characterized by a higher-pressure, lower-temperature assemblage. Although we could not date this event directly in the Chegitun Valley, in the Senyavin uplift (Figure 2) the kyanite-grade event is constrained to have taken place before 132 Ma [*Calvert*, 1999] and was probably due to Late Jurassic–Early Cretaceous deformation during closure of the South Anyui–Angayucham suture. The second event took place at lower-pressure and higher-temperature conditions during deformation accomplished by

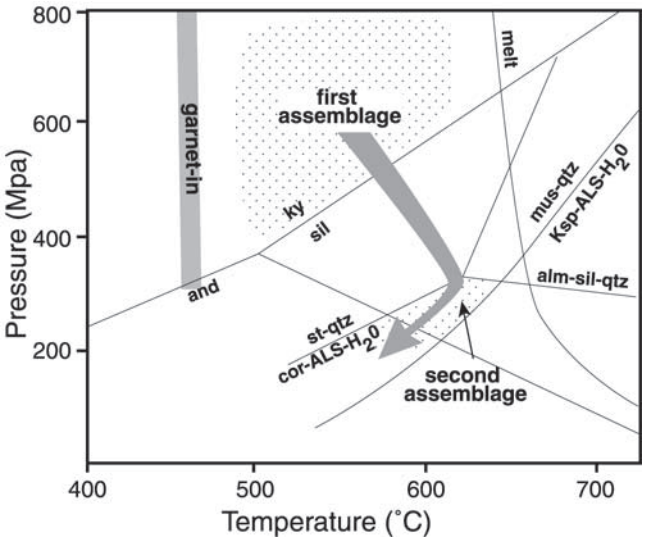

Figure 6. Petrogenetic grid showing the approximate pressure-temperature (P-T) conditions of pelitic schists of the High-Grade unit. The stippled areas show the range of P-T conditions for each assemblage. The first assemblage is characterized by garnet-kyanite, the second assemblage is characterized by syntectonic sillimanite growth after kyanite and cordierite after garnet. The likely P-T path suggests decompression, and perhaps increase of temperature, during development of the dominant fabric (S_{2h}) in the High-Grade unit. Phase boundaries are from *Yardley* [1989]. Abbreviations are as follows: alm, almandine; ALS, aluminosilicate; and, andalusite; cor, cordierite; Ksp, K-feldspar; ky, kyanite; melt, onset of wet melting of granite; mus, muscovite; qtz, quartz; sil, sillimanite; and st, staurolite.

top-to-the-south shear. Thermochronologic data described below demonstrate that this tectonometamorphic event was associated with the mid-Cretaceous development of the Koolen dome. A third, greenschist facies event related to the formation S_{3h} foliation is developed locally. It may be correlated with the greenschist overprint of the high-grade rocks that was observed in the northern margin of the Koolen dome [*Natal'in*, 1979].

3.2. Deformation and Metamorphism in the Tanatap Unit

[17] The Tanatap unit consists of polydeformed, low-greenschist grade, dominantly metasedimentary rocks with minor metavolcanic components. This unit is exposed along most of the Chegitun Valley to the Arctic coast; similar rocks have also been described along the northern flank of the Koolen dome [*Nedomolkin*, 1977; *Natal'in*, 1979].

[18] Three stratigraphic units have been recognized: (1) The Tanatap Formation consists of graphitic phyllite, calcareous slate, marble (limestone turbidites), and massive marble with rare Middle Devonian (Eifelian) fossils [*Nedomolkin*, 1969, 1977; *Oradovskaya and Obut*, 1977; *Krasny and Putintsev*, 1984]. Horizons of andesitic metatuffs are interbedded with the phyllites [*Natal'in et al.*, 1999], as well as rare deformed basaltic dikes of unknown age. (2) The Ikychuren Formation consists of thin bedded marble and calcareous phyllites with rare late Middle Devonian fossils (Givetian). (3) The Utaveem Formation consists of dark fossiliferous marble, calcareous metasandstone, and phyllite of Early Carboniferous age. The tectonic setting and paleogeographic implications of the stratigraphy of the Tanatap unit are discussed by *Natal'in et al.* [1999].

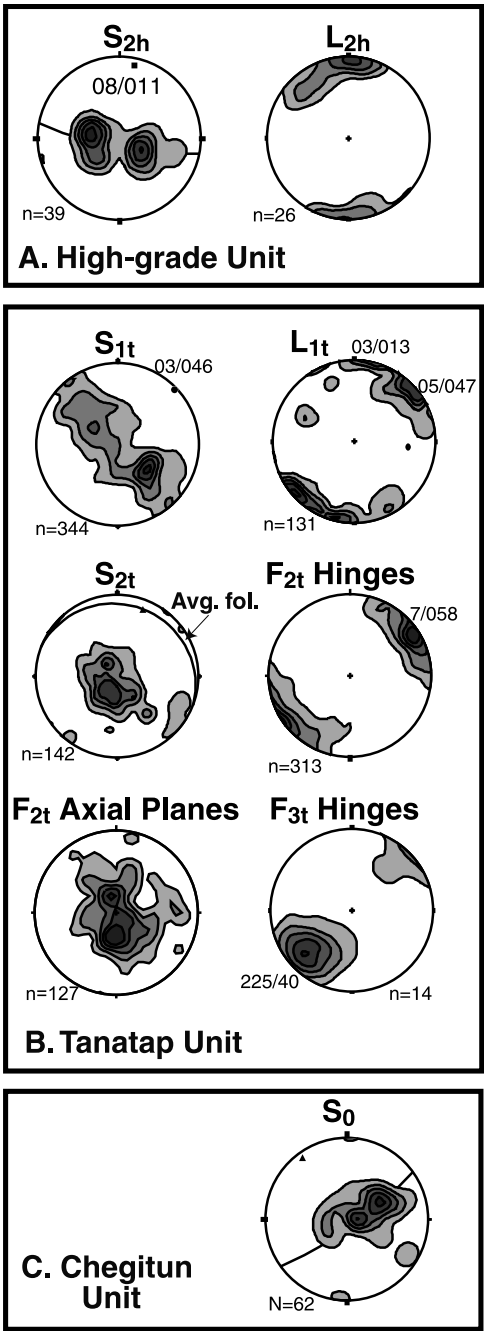

Figure 7. Lower hemisphere stereographic plots of structural data from the Chegitun River valley: (a) High-Grade unit, (b) Tanatap unit, and (c) Chegitun unit.

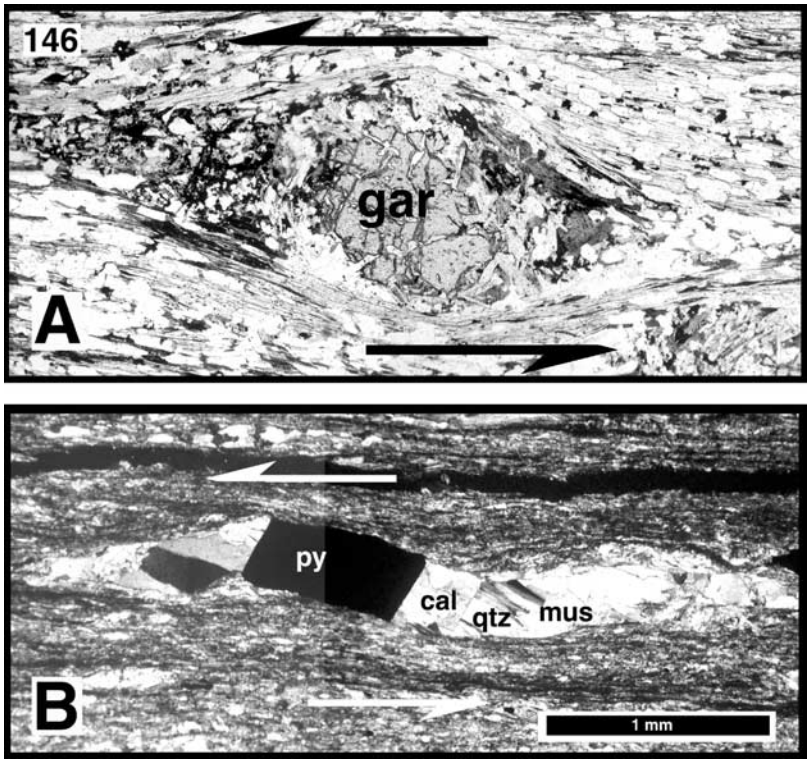

Figure 8. Photomicrographs of shear sense indicators. (a) Garnet porphyroclast with asymmetric stain shadows from Lavrentiya Series pelitic schist in the High-Grade unit. It indicates top-to-the-southeast sense of shear. (b) Pyrite with strain fringes in calcareous phyllite from the Tanatap formation. Fringes are composed of alternating calcite, quartz, and muscovite segments. Length of this fringe relative to the pyrite crystal indicates a minimum stretch of 5.2. Strain fringes with stretches >10 are common in this unit.

[19] Northeast striking rhyolitic dikes intrude the Tanatap unit. These dikes cut the S_{1t} foliation, a fact that constrains them as post-Early Cretaceous and suggests that they are related to the mid-Cretaceous granitic plutons of the Koolen dome. A small granitic stock intrudes the Tanatap Formation north of the Tanatap River (Figure 3).

[20] The Tanatap unit was involved in polyphase deformation (Figure 9b). We recognize four principal phases of deformation. The first phase resulted in the formation of the dominant fabric (S_{1t}), a foliation represented by growth of greenschist facies minerals such as fine-grained white mica, chlorite, actinolite, and albite. This fabric is penetratively developed throughout the Tanatap unit and formed during the peak metamorphic event. S_{1t} developed parallel to the axial plane of isoclinal F_{1t} folds. The dip of the S_{1t} foliation is generally moderate except in the hinges of F_{2t} folds (Figure 7b). Local variations in the attitude of the S_{1t} foliation result from folding during the later stages of deformation. Our thermochronologic data, detailed below, indicate that the S_{1t} fabric formed prior to 117 Ma.

[21] The L_{1t} lineation that developed on S_{1t} foliation planes is represented by elongate mineral aggregates (calcite, quartz, mica, chlorite, and pyrite), by strain fringes around pyrite (Figure 8b), by individual minerals such as actinolite, and by stretched pebbles in debris flow deposits. The L_{1t} lineations generally trend NE-SW or N-S (Figure 7b). Sense of shear deduced from asymmetric strain shadows and mica fish is generally top to the south in the central and southern part of the map area, but in other areas, sense of shear is variable perhaps due to reverse shearing, which commonly develops during low-grade metamorphism [*Hippert and Tohver*, 1999].

[22] The second phase of deformation (D_{2t}) resulted in dramatic tight, recumbent F_{2t} folds, as well as axial plane cleavage S_{2t}, and intersection lineations L_{2t}. These fabric elements clearly overprint the earlier foliation S_{1t} and lineation L_{1t}. The second foliation (S_{2t}), which is not developed in the northernmost and southernmost parts of the Tanatap unit, consists of spaced cleavage planes, crenulation cleavage, and in rare cases new white mica growth. The S_{2t} cleavage is generally subhorizontal indicating that it developed with an important component of vertical flattening (Figure 7b). The S_{2t} cleavage changes orientation from south to north through the central part of the Tanatap unit. It first dips gently to the northeast, and then it dips to the north and finally to the northwest (Figure 9a). We interpret these changes in S_{2t} cleavage attitude to be the result of folding during right-lateral movement along the Ratkhat fault during the last stage of deformation (D_{4t}).

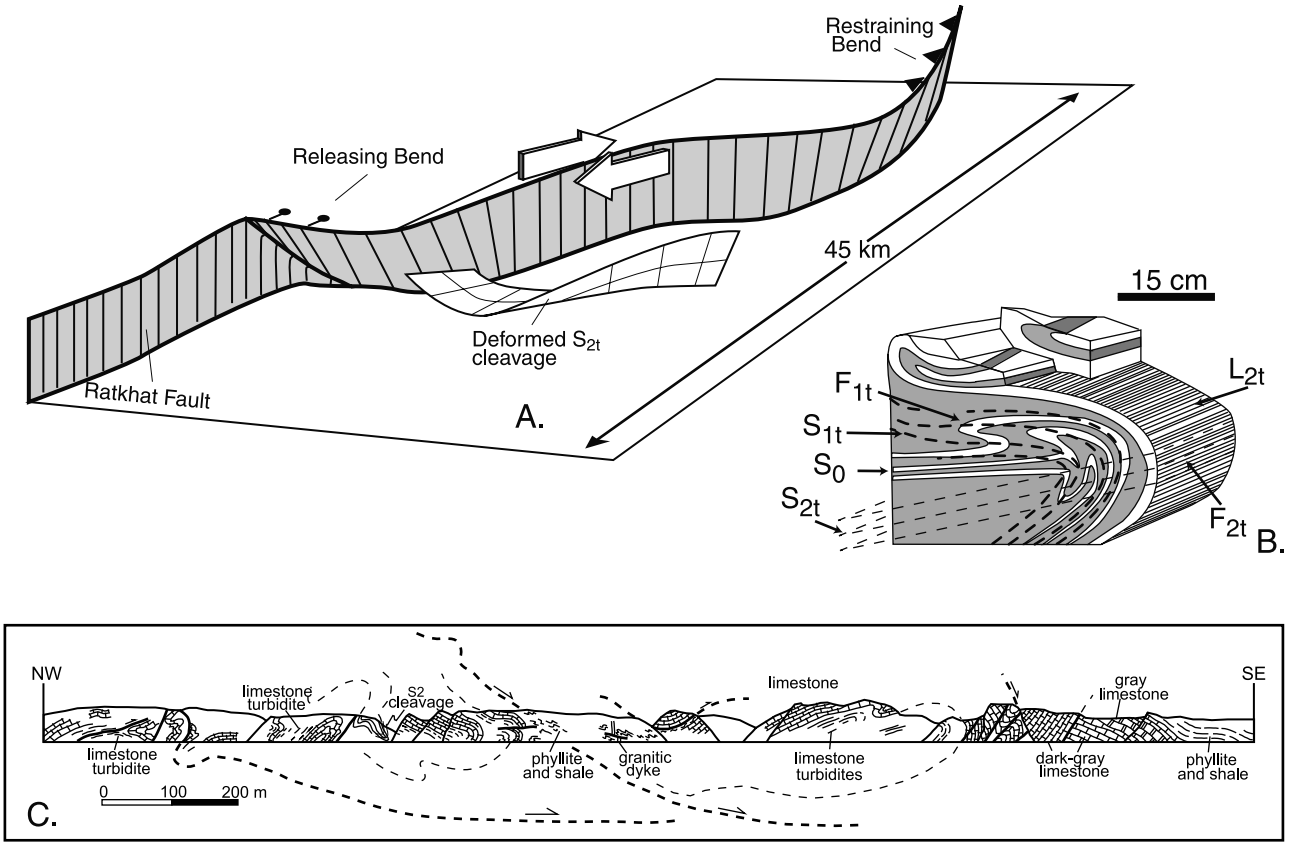

Figure 9. Schematic drawings of the fabrics and structures within the Tanatap unit. (a) Cartoon representing the relationship between the likely shape of the fault plane of the Ratkhat fault and structures associated with it, including the extensional structures within the Chegitun unit in the southern part of the map area, compressional structures in the northern part of the map area, and regional changes in attitude of the S_{2t} cleavage in the Tanatap unit (modified after *Natal'in* [1999]). (b) Sketch of a small-scale fold (F_{2t}) that refolds the S_{1t} fabric. Although F_{2t} folds are widespread, the S_{2t} cleavage is not always developed. (c) The F_{3t} folds in cliffs along the Tanatap River Valley. Note northwestward vergence and folding of the S_{2t} cleavage.

In general, the hinges of F_{2t} folds and L_{2t} intersection lineations are subhorizontal and northeast trending (Figure 7b). They are typically parallel to L_{1t} lineation although locally a rotation of L_{1t} lineations around the hinges of F_{2t} folds can be found. F_{2t} folds often exhibit asymmetric profiles with predominantly southeastern vergence irrespective of the orientation of S_{1t}. We attribute the D_{2t} fabrics to extensional deformation of the flank of the Koolen dome coeval with development of the dominant fabric in the High-Grade unit.

[23] Large recumbent folds (F_{3t}) that involve the S_{2t} cleavage are locally developed in several places of the Tanatap unit (Figure 9c). Hinges of the folds are subparallel to the F_{2t} hinge lines and L_{1t} lineation, though in places oblique relationships were observed. Scattering of poles to axial planes of the F_{2t} folds along a northeast striking great circle girdle (Figure 7b) may be attributed to F_{3t} folding. The F_{3t} folds are linked to gently dipping faults. Both fold vergence and fault slip direction indicate northward tectonic transport, that is, almost opposite to the predominant sense of vergence of F_{2t} folds and opposite to the sense of shear of L_{2h} in the High-Grande unit. Zones of late-stage antithetic deformation develop in core complexes when uplift of the dome folds the detachment creating a zone that dips back toward the break-away fault [*Reynolds and Lister*, 1990]. Thus uplift of the core of the Koolen dome may account for the F_{3t} folds of the Tanatap unit.

[24] The fourth phase of deformation (D_{4t}) created open folds superimposed on all earlier fabrics. F_{4t} folds of meter- to decimeter-scale are common, and larger folds can be inferred from the map pattern. The outcrop-scale folds have moderately SW plunging hinges and are superimposed upon S_{1t} and S_{2t} foliations. Most of these folds have asymmetric profiles that show a right-lateral component of shearing in regional planes of S_{2t} foliation.

[25] There are also brittle normal, reverse, and strike-slip faults that cut both the Tanatap and the Chegitun units. All these faults, as wells as the F_{4t} folds, can be accounted for by a single late-stage episode of right-lateral deformation that also produced the Ratkhat and Nynykin faults which bound the Tanatap unit (Figures 3, 4, and 9a). These two faults are seldom exposed, but their regional importance is

evident from the map patterns, the truncation of structural trends at the edge of each of the lithotectonic unit (Figure 3), and the abrupt juxtaposition of disparate metamorphic grades and structural styles. We deduced the kinematics of these faults on the basis of secondary structures, including variations of the orientation of S_{2t} cleavage, and zones of transtension and transpression near bends in the strike-slip faults (Figure 9a). Detailed description of these structures is given by *Natal'in* [1999].

3.3. Deformation in the Chegitun Unit

[26] The Chegitun unit consists of shallow marine Middle Ordovician to Lower Devonian limestones, dolomites, and minor shales [*Oradovskaya and Obut*, 1977; *Natal'in et al.*, 1999]. The oldest exposed unit is the Isseten Formation (Middle Ordovician), which consists of 430–540 m of fossil-rich dark gray to gray limestone and limestone breccia. These rocks are overlain by the Chegitun Formation (Upper Ordovician), which is represented by 225–350 m of dark gray bioclastic and reefal limestone and dolomite. Above the Chegitun Formation lies the Putukuney Formation (Silurian), which is only 60–70 m thick. The dominant lithologies are calcareous black shale and flaggy argillaceous limestone. These are conformably overlain by 300–315 m of grey to yellow massive dolomite of the Orlan Formation (Late Silurian). The youngest strata exposed are dolomitic limestones with stromatoporoid corals (Lower Devonian) which are ~250 m thick.

[27] The Chegitun unit is devoid of metamorphic minerals or penetrative cleavage. Bedding is gently to moderately dipping and is cut by high-angle faults. Thus the internal structure of the unit is very different from that of the High-Grade and Tanatap units. The transition between the complex structural style of the Tanatap unit and the very simple structural style of the Chegitun unit is abrupt. The Ratkhat fault has juxtaposed a portion of the upper plate of the Koolen extensional complex, represented by the Chegitun unit, with deeper structural levels represented by the Tanatap unit.

[28] Despite the lack of new mineral growth within the Chegitun unit, conodonts recovered from the Chegitun and Orlan Formations have alteration indices ranging from 5 to 6 (A. Harris, written communication, 1997). According to the experiments of *Rejebian et al.* [1987] these indices correspond to paleotemperatures of 300°C–435°C. These high paleotemperatures could have been attained by sedimentary and tectonic burial, perhaps during closure of the South Anyui suture or by heating during mid-Cretaceous intrusion of the granitic suite of the Koolen and Neshkan metamorphic domes that flank the Chegitun unit on both sides (Figure 2).

[29] Folds in the Chegitun unit are open with wavelengths of hundreds of meters to kilometers. The folds have predominantly NW trending axes as indicated by the distribution of poles to bedding (Figure 7c). Although the thickness of the stratigraphic units determined by *Oradovskaya and Obut* [1977] are generally confirmed by our observations and cross sections (Figure 4, cross section C-C′), there are some local discrepancies. For example, the Upper Ordovician Chegitun Formation appears to dip homoclinally to the west in the northern part of the map area. If this section is continuous, the implied stratigraphic thickness is more than double the normal thickness of the unit. A similar situation arises in the southern part of the map area. It is likely that unmapped thrust faults, related to the D_1 event in the Tanatap and High-Grade units, duplicate parts of these sections.

[30] Two sets of faults cut the Chegitun unit [*Natal'in*, 1999]. The first set consists of moderately to steeply dipping NW striking normal faults (Figures 3 and 4). All studied faults dip to NE; striation, mineral fibers, tension gaps, and Riedel shears indicate downdip sense of motion on these faults. *Nedomolkin* [1969, 1977] mapped several steep northwest trending faults providing no information on their kinematic history. We interpret these faults as northeast dipping normal faults based on the age relationships of juxtaposed strata.

[31] The second set of faults includes northeast striking faults mapped within the Chegitun unit by *Nedomolkin* [1977] (Figure 3). These faults are parallel to the Ratkhat right-lateral strike-slip fault, and therefore we infer a similar kinematic history.

4. Geochronology

[32] We carried out $^{40}Ar/^{39}Ar$ analyses on hornblende and mica samples from both Etelkhvyleut and Lavrentiya Series of the High-Grade unit, and from metamorphic rocks in the Tanatap unit, in order to evaluate the timing of metamorphism and subsequent cooling history. The analyses were performed at Stanford University under the supervision of M. McWilliams. Description of the analytical procedures and sample preparation techniques are given by *Hacker and Wang* [1995]. The full isotopic data set, as well as all the spectra, inverse isochrons are available in the auxiliary material.[1] Few of the ages reported below fit the strict definition of a plateau age [*Dalrymple and Lanphere*, 1974]. In most cases we use the weighted mean age of the relatively flat, continuous portion of each spectrum.

4.1. High-Grade Unit

[33] Hornblende from Etelkhvyleut Series amphibolites (sample 95JT5a, see Figure 3 for location) yielded a weighted mean age of 109 ± 1 Ma with an $^{40}Ar/^{36}Ar$ ratio within error of the expected atmospheric ratio (295.5) (Figure 10a and Table 1). Biotite from the same sample produced a weighted mean age of 104 ± 1 Ma. Muscovite from a biotite-muscovite-garnet quartzite of the Lavrentiya Series (sample 95JT16) yielded a plateau age of 109 ± 1 Ma (Figure 10b, Table 1). This age is very reliable because the total fusion age, plateau age, and isochron age are all within error of each other, and the $^{40}Ar/^{36}Ar$ intercept of the isochron plot is indistinguishable from the atmospheric

[1] Auxiliary material is available via Web browser or via Anonymous FTP from ftp://ftp.agu/append/tc/2001TC001333. Information on searching and submitting electronic supplements is found at http://www.agu.org/pubs/esupp_about.html.

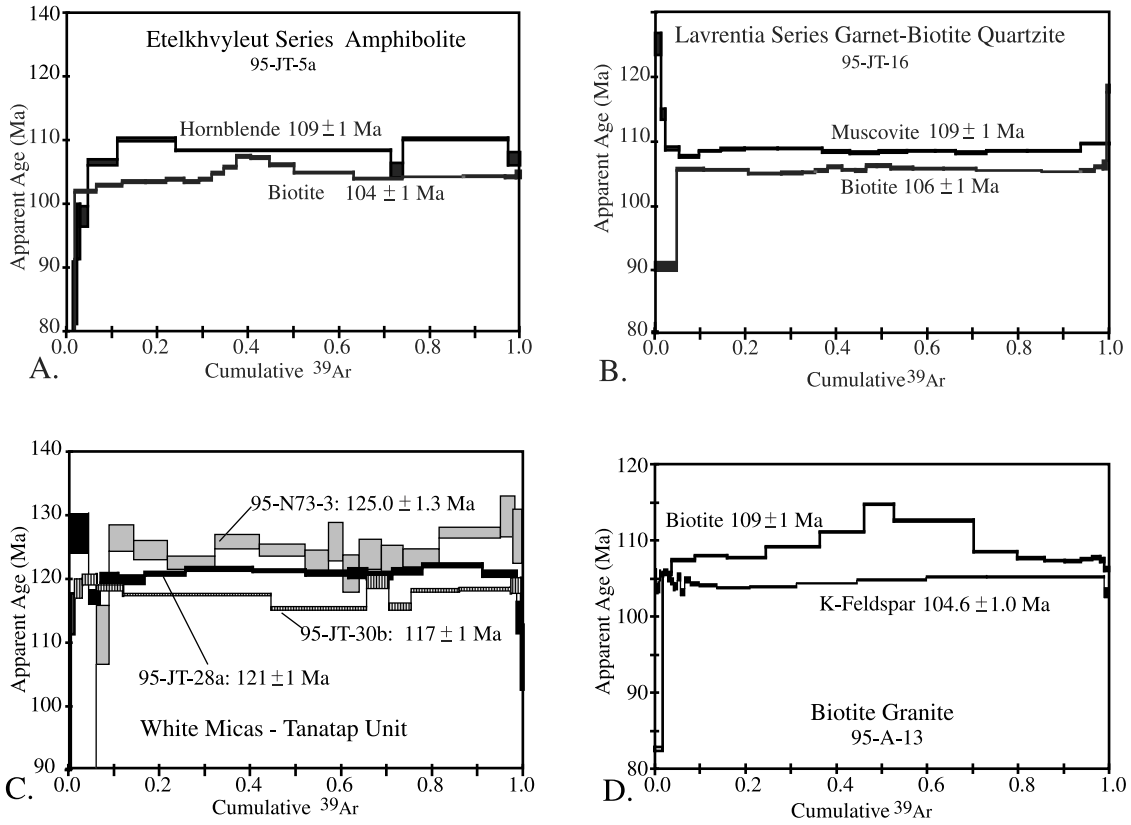

Figure 10. The $^{40}Ar/^{39}Ar$ spectra from the Chegitun Valley. Ages given are weighted mean ages calculated from the relatively flat portions of each spectrum. See Table 1 for details. (a) Spectra from hornblende and biotite from amphibolite of the Etelkhvyleut Series of the High-Grade unit. (b) Spectra from micas in quartzite of the Lavrentiya Series of the High-Grade unit. (c) Spectra from white micas of the Tanatap unit. (d) Spectra from biotite and K-feldspar in granite stock that intrudes the Tanatap unit.

Table 1. Summary of $^{40}Ar/^{39}Ar$ Data From the Chegitun River Area[a]

Sample	Lithology	Mineral	Latitude, N	Longitude, W	Total Fusion Age, Ma	Isochron Age, Ma	MSWD	$^{40}Ar/^{36}Ar$	WM Age, Ma	Steps Used[b]	^{39}Ar Used, %
					High-Grade Unit						
95JT5a	amphibolite	hornblende	66°13.99′	171°55.52′	107.4 ± 1.2	109.0 ± 1.2	28	304 ± 25	109.1 ± 1.1	7–11/11	88
95JT5a	amphibolite	biotite	66°13.99′	171°55.52′	103.0 ± 1.0				104.3 ± 1.0	2–19/19	98
95JT16	gar mica quartzite	white mica	66°17.23′	171°50.58′	108.9 ± 1.0	108.6 ± 1.0	11	291 ± 17	108.6 ± 1.0	3–17/17	97
95JT16	gar mica quartzite	biotite	66°17.23′	171°50.58′	104.9 ± 1.0	105.3 ± 1.0	5.8	326 ± 20	105.5 ± 1.0	2–20/21	95
					Tanatap Unit						
95JT28a	calc phyllite	white mica	66°21.12′	171°38.28′	121.0 ± 1.2	121.3 ± 1.2	3.76	292 ± 34	121.2 ± 1.2	3–13/15	91
95JT30b	calc phyllite	white mica	66°20.27′	171°40.89′	117.2 ± 1.1	117.5 ± 1.2	15.5	283 ± 12	117.3 ± 1.1	1–12/13	99
95N73-3	calc silicate	white mica	66°20.29′	171°36.95′	122.0 ± 1.3	127.1 ± 2.3	1.8	284 ± 10	124.9 ± 1.3	3–16/16	91
					Intrusive Rocks						
95A13	granite	biotite	66°20.98′	171°32.80′	109.1 ± 1.1	109.3 ± 1.3	601	297 ± 49	109.2 ± 1.0	2–17/17	98
95A13	granite	K feldspar	66°20.98′	171°32.80′	104.7 ± 1.0	105.4 ± 1.0	5.7	286 ± 2	104.6 ± 1.0	2–22/24	99

[a]Definitions are as follows: MSWD, mean square weighted deviation, a measure of the goodness of fit of the isochron [*Wendlt and Carl*, 1991]; WM Age, weighted mean age calculated from the relatively flat portion of the spectrum; and Steps Used and ^{39}Ar Used (%), heating steps used to calculate the weighted mean age.

[b]The following is a summary of key laboratory procedures. Clean 1–5 mg of each mineral sample were packaged in Cu or Al foil and irradiated at the TRIGA reactor at the University of Oregon. The analyses were carried out at the laboratory of M. McWilliams at Stanford University. The laboratory equipment used and analytical procedures followed are those described by *Hacker and Wang* [1995]. The mass spectrometer data were corrected for neutron flux gradient using the sanidine standard 85G003 with assumed age of 27.92 Ma. All the analyses were corrected for decay since irradiation, mass discrimination, and interference of Cl-, Ca-, and K- produced Ar isotopes. Uncertainties reported are 1σ, determined using the uncertainties in monitor age, decay rates of ^{37}Ar, ^{39}Ar, and ^{40}Ar, rates of reactor-produced Ar isotopes, duration of irradiation, time since irradiation, peak heights, blank values, and irradiation parameter *J*.

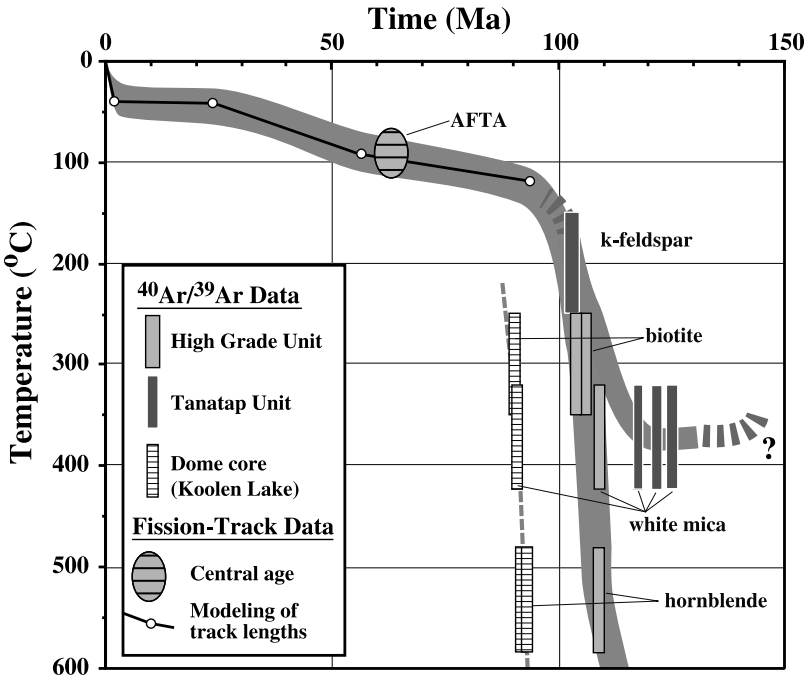

Figure 11. Cooling history of the Koolen dome based on $^{30}Ar/^{39}Ar$ data and modeling of one apatite fission track age. The cooling history of the core of the dome is based on thermochronologic work of *Akinin and Calvert* [2002] in the Koolen Lake area. The Tanatap unit preserves evidence of an Early Cretaceous thermal event. Rapid cooling in the High-Grade unit is associated with the development of the Koolen dome. The NW flank of the dome cooled ~12 Myr before the core.

ratio. Biotite from the same sample produced a reliable weighted mean age of 106 ± 1 Ma.

[34] We conclude that these $^{40}Ar/^{39}Ar$ ages date postmetamorphic cooling of the rocks because the peak temperature implied by their metamorphic assemblages (Figure 6) exceeds the Ar closure temperature of hornblende (535°C ± 50°C [*Harrison*, 1981]). It is notable that both the age of hornblende from the Etelkhvyleut Series amphibolite and that of white mica from the Lavrentiya Series are ~5 Ma older than the peak metamorphism in the core of the dome as determined by *BSGFP* [1997] and *Akinin and Calvert* [2002]. Furthermore it appears that the rocks had cooled below the closure temperature of biotite (335°C ± 50°C [*Harrison et al.*, 1985; *Grove and Harrison*, 1996]) by 104 Ma, while peak metamorphic conditions prevailed in the core (Figure 11). Therefore cooling of the dome, which presumably occurred during exhumation, was diachronous, with the northwestern flank moving upward in the crust while the core continued to experience upper amphibolite-facies conditions.

[35] One apatite fission track age from a granitic orthogneiss of the Etelkhvyleut Series was determined by T. Dumitru at Stanford University (sample 95JT4a, Tables 2a and 2b). The age of the sample was 63 ± 3 Ma, and it had a negatively skewed track-length distribution with a mean length of 12.9 ± 0.2 mm. The apatite fission track method dates cooling through ~110°C to 60°C, the range of temperatures over which fission tracks become annealed [*Gleadow et al.*, 1986]. Residence within this temperature range causes the tracks to shorten progressively from their initial mean length of ~16 mm; therefore the age and track-length distribution of a sample are the product of the cooling history. For a full description of the analytical methods, refer to *Dumitru et al.* [1995].

[36] The fission track age from the Etelkhvyleut Series augen gneiss demonstrates that the High-Grade unit had been exhumed to within a few kilometers of the surface by latest Cretaceous time. The fact that the tracks in sample 95JT4a are significantly shortened indicates that cooling through the 110°C–60°C range was slow. This is confirmed by modeling of the age and track-length distribution using the methods of *Gallagher* [1994]. The best fit thermal history is incorporated into the thermal history of the High-Grade unit (Figure 11).

4.2. Tanatap Unit

[37] We carried out $^{40}Ar/^{39}Ar$ age determinations of three white mica samples from metamorphic rocks of the northern part of the Tanatap unit (see Figure 3 for locations). The oldest age (125 ± 1 Ma) was obtained from sample 95N73-3, a coarse-grained, calcite-white mica-biotite-albite-epidote bearing calc-silicate rock. The protolith was probably a mafic dike or sill that intruded limestones of the Ikychuren Formation. The host rocks reveal a weak S_{1t} foliation, but the calc-silicate rock is rather massive. The white mica from this rock has low K/Ca (<1.5) and might be margarite (Ca-mica) or paragonite (Na-mica). The argon content is low, but validity of these data is supported by the

Table 2a. Apatite Fission Track Data for Sample 95JT4a

Parameter	Value
Localities, Counting, Age Data	
Latitude, N	66°14.1′
Longitude, W	171°55.78′
Elevation, m	120
Individual grains dated	33
Spontaneous track density, $\times 10^6$ tracks/cm^2	0.61
Spontaneous tracks counted	650
Induced track density in external detector (muscovite), $\times 10^6$ tracks/cm^2	3.125
Induced tracks counted	3327
χ^2 probability,[a] %	21
Dosimeter, track density,[b] $\times 10^6$ tracks/cm^2	1.653
Dosimeter, tracks counted	4933
Age ± 1σ,[c] Ma	63.2 ± 3.3
Length Data Statistics	
Mean length	12.94 ± 0.2 μm
Standard deviation	2.478
Skewness	−1.602
Kurtosis	2.374
Number	150

[a]See *Galbraith* [1981] and *Green* [1981].
[b]External detector is adjacent to CN5 dosimetry glass.
[c]Age is the sample fission track central age [*Galbraith and Laslett*, 1993], calculated using zeta calibration method [*Hurford and Green*, 1983] with zeta of 385.9 for CN5. Details of the laboratory procedures are given by *Dumitru et al.* [1995].

fact that the isochron age is concordant with the weighted mean age of 125 ± 1 Ma (Figure 10c) and the $^{40}Ar/^{36}Ar$ is the same as the atmospheric ratio (Table 1). This age dates metasomatism of the mafic protolith that appears to be slightly older than the D_{1t} deformation in the Tanatap unit.

[38] Muscovite was extracted from an albite-white mica bearing calcareous phyllite of the Tanatap Formation (sample 95JT28a). The phyllite has a well-developed S_{1t} foliation defined by the growth of muscovite and a weakly developed S_{2t} spaced pressure-solution cleavage. The experiment yielded a flat spectrum with a weighted mean age of 121 ± 1 Ma that is concordant with the isochron and total fusion age (Figure 10c and Table 1). The $^{40}Ar/^{36}Ar$ ratio is also atmospheric. Therefore rocks of the Tanatap unit had cooled below closure temperature of muscovite (370°C ± 50°C [*Lister and Baldwin*, 1996]) by this time. Owing to the low grade of these rocks it is unlikely that they experienced temperatures above the muscovite closure temperature. Therefore this Early Cretaceous $^{40}Ar/^{39}Ar$ age approximates the age of the earliest deformation and metamorphism in the Tanatap unit (D_{1t}).

[39] We extracted S_{1t} muscovite from a crenulated phyllite of the Tanatap Formation (sample 95JT30). Although S_{2t} crenulations are strongly developed, there is no muscovite growth associated with the D_{2t} event. The sample yielded a weighted mean age of 117 ± 1 Ma, which is concordant with the total fusion age and the isochron age, although there are several discordant steps in the spectrum (Figure 10 and Table 1). The $^{40}Ar/^{36}Ar$ ratio of the experiment is atmospheric. This age is significantly younger than the 121 Ma age of sample 95JT28a. This might be due to disturbance of the isotopic system during the D_{2t} event, or it may indicate diachronous white mica growth during the D_{1t} event.

[40] We also dated two mineral separates from the small biotite-bearing granite that intrudes the Tanatap unit east of the Tanatap River (sample 95A13, Figure 3). The granite appears to be undeformed in hand specimen, but in thin section, there is evidence for incipient ductile deformation. Quartz grains have undulose extinction or are broken into subgrains. Quartz grain boundaries are lobate, indicating active grain boundary migration. K-feldspars display deformation bands and flame-perthite texture. In addition, K-feldspars often have a thin mantle of fine recrystallized grains. These textural observations indicate that the granite underwent deformation at low- to medium-grade conditions (400°C–500°C [*Passchier and Trouw*, 1996]) and then cooled before annealing could ensue. Biotite from this granite sample yielded a spectrum with a central "hump." The weighted mean age calculated excluding the anomalously old steps is 108 ± 1 Ma. The older steps form a linear array on the inverse isochron plot with a $^{40}Ar/^{36}Ar$ intercept of 1129 ± 314, indicative of the incorporation of excess radiogenic Ar. Although the exact age of crystallization of this granite is unknown, it is notable that this biotite $^{40}Ar/^{39}Ar$ age is coeval with the $^{40}Ar/^{39}Ar$ hornblende cooling ages, which probably approximate peak metamorphic conditions in the High-Grade unit.

[41] K-feldspar from the same granite sample yielded a spectrum that after some disturbed low-temperature steps rises from 103 Ma to 105 Ma with a weighted mean age of 104.6 ± 1.0 Ma (Figure 10d). K-feldspars do not have a unique closure temperature. Instead, multiple diffusion domains retain argon to different degrees, and it is necessary to determine the kinetic parameters of each sample from the $^{40}Ar/^{39}Ar$ analysis [*Lovera et al.*, 1989]. Although our analysis was not designed to carry out the detailed modeling that can determine the specific cooling history of the sample, the data suggest that the granite cooled from above ~250°C to below ~150°C between 105 and 103 Ma.

[42] In summary, $^{40}Ar/^{39}Ar$ dating of the Tanatap unit demonstrates that the S_{1t} foliation formed before 117 Ma, and the D_{1t} event may have already been in progress by 125 Ma.

Table 2b. Track-Length Distribution for Sample 95JT4a

Binned Lengths, μm	Number of Tracks
3–4	1
4–5	1
5–6	2
6–7	1
7–8	6
8–9	5
9–10	2
10–11	6
11–12	8
12–13	21
13–14	33
14–15	48
15–16	12
16–17	4

Development of the S_{2t} fabric took place at low enough temperatures that there was neither significant growth of new minerals nor resetting of the older ages within the Tanatap unit, yet the rocks were intensely deformed. Although we were unable to date the S_{2t} fabric directly, we correlate it with the dominant S_{2h} of the High-Grade unit and with development of the Koolen dome. Petrographic observations and $^{40}Ar/^{39}Ar$ thermochronologic data from the small granite pluton that intrudes the Tanatap unit suggests that ductile deformation was waning by 109 Ma with exhumation of the Tanatap unit into the upper crust by 103 Ma. This gives us the rough estimation of the age of D_{2t} and, perhaps, D_{3t} episodes that were ductile in their nature.

5. Discussion

[43] The Mesozoic structural history of the Chegitun Valley encompasses three main deformational episodes that are differently expressed in each of the lithotectonic units of the area. These events are summarized below with reference to both their expression in the Chegitun Valley and their regional implications. These events include (1) Early Cretaceous collision along the South Anyui–Angayucham suture; (2) development of the mid-Cretaceous metamorphic complexes; and (3) Late Cretaceous–Tertiary strike-slip and normal faulting.

5.1. Collision of Chukotka–Arctic Alaska

[44] The earliest deformation in the Chegitun Valley area is best represented by the S_{1t} fabric in the Tanatap unit. According to our $^{40}Ar/^{39}Ar$ data this event occurred before 117 Ma and extended at least as far back as 124 Ma (late Neocomian). These ages are significantly older than those determined from the High-Grade unit either within our field area or in the core of the dome [*BSGFP*, 1997; *Calvert*, 1999]. It is likely that the D_{1t} deformation was related to the regional collisional event along the South Anyui–Angayucham suture [*Natal'in and Toro*, 1998; *Natali'n et al.*, 1998]. Evidence from western Chukotka indicates that this collision took place at the end of the Neocomian, between ~130 and 124 Ma [*Natal'in*, 1984]. Evidence for this event also exists in the Seward Peninsula of Alaska, where relict blueschist facies assemblages are common in the Nome Group [*Patrick and Evans*, 1989]. The $^{40}Ar/^{39}Ar$ dating of white mica from the Nome Group suggests that high-pressure/low-temperature metamorphism associated with this event took place before 120 Ma [*Hannula et al.*, 1995]. In the Brooks Range, rocks of the Chukotka–Arctic Alaska continental margin underwent high-pressure/low-temperature metamorphism at ~149–129 Ma [*Gottschalk and Snee*, 1998]. Therefore the D_{1t} deformation in the Chegitun Valley represents the final stages of polyphase collisional deformation along the South Anyui suture. The direction of tectonic transport associated with L_{1t} lineation was parallel to the general strike of the Tanatap and Chegitun units. Both units have great lateral extend [*Natal'in et al.*, 1999]. One of us (B. Natal'in) interprets the parallelism of the L_{1t} lineation and the boundary of these units along a distance of 25 km as the evidence for orogen-parallel tectonic transport. If this conclusion is correct, the D_{1t} deformation may be correlated with the suture-parallel shearing established in the South Anyui Range [*Natal'in*, 1984; *Sokolov et al.*, 2002].

[45] Our preferred interpretation is that the relict kyanite-bearing assemblage found in the High-Grade unit formed during high-pressure/moderate-temperature metamorphism associated with the same collisional event. This interpretation is supported by the existence of 132 Ma, or older, kyanite-bearing assemblages in the Senyavin uplift of southern Chukotka Peninsula. There moderate-pressure metamorphism was attributed to thrust emplacement of oceanic rocks onto the continental margin during closure of the South Anyui–Angayucham suture [*Calvert*, 1999]. Although relict kyanite in the High-Grade unit is preserved, the $^{40}Ar/^{39}Ar$ system in the High-Grade unit was completely reset during mid-Cretaceous development of the Koolen dome and the associated magmatic heating. In contrast, the rocks of the Tanatap unit remained cool enough to retain the ages of the Early Cretaceous metamorphic event. Alternatively, the kyanite-bearing assemblages could have formed during the Paleozoic evolution of the Devonian arc-trench system, parts of which are represented by the Tanatap unit and Devonian granitoids in the High-Grade unit [*Natal'in et al.*, 1999]. It will be necessary to date kyanite-bearing assemblage directly in order to choose between these two interpretations with certainty.

5.2. Formation of the Mid-Cretaceous Metamorphic Complexes

[46] On the basis of our structural and geochronologic data we link the dominant metamorphic fabric in the High-Grade unit (S_{2h}) and the D_{2t} fabrics of the Tanatap unit with the mid-Cretaceous development of the Koolen metamorphic complex. Two hypotheses have been proposed to explain the genesis of the dome. In one model [*BSGFP*, 1997] the sillimanite-grade rocks of the core of the dome were exhumed during north-south extension of the Bering Sea region and accompanied by magmatic heating and solid-state flow of the middle and lower crust. An alternative model proposes thermally driven diapiric rise of the high-grade rocks, followed by local extensional faulting [*Parfenov and Natal'in*, 1979; *Akinin and Calvert*, 2002].

[47] Our structural data from the High-Grade unit combined with data presented by *BSGFP* [1997] are confined to a transect that starts from the northwestern flank of the Koolen dome and passes through its core and southern flank extending almost to the southern edge of the dome. These data suggest that high-strain ductile deformation took place within a top-to-the-south shear regime with some notable deviations to the southeast in the core and near the southern edge. This argues for a unidirectional core complex-type geometry and argues against a diapiric model that would produce a more radial pattern of deformation [*Natal'in and Toro*, 1998]. The thermochronologic data from the Koolen dome, which admittedly are limited in geographic extent (Figure 2), also support this conclusion. The NW flank of the Koolen dome cooled from 500°C to 300°C between 109 and 104 Ma, while cooling in the core of the dome started at 94 Ma (Figure 11) [*Akinin and*

Calvert, 2002]. The central part of a diapir would be the first to rise through the crust and cool down. In contrast, if cooling was driven by tectonic denudation, the areas near the breakaway zone of the detachment would cool before the center of the dome.

[48] What was the driving mechanism for the development of the Koolen dome? Collapse of overthickened continental crust [*England*, 1983; *Dewey*, 1988] has been proposed as one of the mechanisms for extensional deformation [*Natal'in and Toro*, 1998]. Thermobarometry of the Koolen complex shows that rocks found in the center of the dome experienced pressures of up to 700 MPa in the mid-Cretaceous [*Akinin and Calvert*, 2002]. If we assume a lithostatic pressure and granitic composition for the upper crust, this yields a paleodepth of ~27 km. The current crustal thickness in the Bering Strait region is ~32 km as determined from deep-crustal seismic reflection and refraction experiments [*Klemperer et al.*, 2002]. Therefore crustal thickness must have been at least 59 km prior to exhumation. This figure is only a minimum because it does not take into account thinning of the lower crust by ductile flow, which is evidenced by intense lower crustal reflectivity in the Bering Strait [*Klemperer et al.*, 2002]. A crustal thickness of >59 km makes the mid-Cretaceous Bering Strait region a good candidate for gravitational collapse.

[49] However, this cannot be the sole explanation for the origin of the Koolen dome. Although Early Cretaceous collision affected the entire length of the Chukotka-Alaska Chukotka block, the metamorphic complexes are only found in the Bering Strait region. It has been demonstrated that there is a close temporal linkage between subduction-related magmatism and intense ductile deformation in the domes both in Chukotka [*BSGFP*, 1997] and in Alaska [*Amato et al.*, 1994; *Amato and Wright*, 1998]. Therefore the mid-Cretaceous metamorphic domes are found where the Early Cretaceous collisional belt was located over the paleo-Pacific subduction zone. Magmatic heating would have weakened the lower and middle crust promoting extensional collapse, as has been proposed for the Cordilleran core complexes [*Coney and Harms*, 1984].

[50] An additional peculiarity of the Bering Strait region is the sinuosity of structural trends (Figure 1), which has been attributed to oroclinal bending [*Natal'in and Parfenov*, 1976; *Patton and Tailleur*, 1977; *Plafker and Berg*, 1994]. The Bering Strait orocline (also known as the Chukchi syntaxis) helps to account for the great crustal thickness that existed in the Bering region during the Early Cretaceous. An impressive collisional event has been documented in northern Alaska where the Koyukuk arc collided with Arctic Alaska passive continental margin [e.g., *Moore et al.*, 1994a, 1994b]. However, in Chukotka the collision was not as strong. This inference follows from the absence of foredeep basins in western Chukotka, the short time span of contraction, orogen-parallel strike-slip displacements that accompanied the collision, and the normal crustal thickness found along the portion of the South Anyui suture that has not been affected by extension [*Gramberg and Pogrebitzkiy*, 1984].

[51] Formation of the Bering Strait orocline has been related to dextral displacements on major strike-slip faults in Alaska [*Plafker and Berg*, 1994] and sinistral displacements along NW striking faults in Chukotka [*Natal'in and Parfenov*, 1976]. The ages of the Alaskan strike-slip faults suggest that the orocline is Late Cretaceous–Tertiary in age [*Plafker and Berg*, 1994]. However, in Chukotka the formation of orocline-related faults started prior to the Middle to Late Cretaceous Okhotsk-Chukotka volcanic belt as it is evidenced from overlapping relationships with the Okhotsk-Chukotka magmatic belt [*Natal'in*, 1984]. The Late Cretaceous Okhotsk-Chukotka belt is less affected by oroclinal bending. If the South-Anyui-Angayucham suture is taken as a reference (Figure 1), the amount of shortening in the orocline core could be up to 180%. This amount of shortening roughly fits the estimation of crustal thickness of 58 km that we deduced from the thermobarometry of the Koolen metamorphic complex and the present day crustal thickness. Thus we infer that the formation of the Bering Sea orocline was responsible for east-west shortening that contributed to thickening the crust in the Bering Strait region and helps explain why metamorphic core complexes do not exist along the entire length of the South Anyui–Angayucham suture.

[52] *Rubin et al.* [1995] pointed out that during the 130–80 Myr time span, concurrent with southward rotation of the Chukotka–Arctic Alaska block, the paleosubduction zone must have retreated out of the Arctic as well. They proposed that extensional deformation above the subduction zone was the result of trench retreat. However, the detailed time-space distribution of mid-Cretaceous magmatism in the region is very complex and defies a simple model of southward migration. For example, in the Bering Strait region, Early Cretaceous plutons, which predate the formation of the metamorphic complexes, are exposed closer to the paleosubduction zone than the Late Cretaceous magmatic arc, which postdates the metamorphic complexes [*Parfenov and Natal'in*, 1985; *Miller*, 1994]. This movement of the magmatic front away from the subduction zone contradicts the trench rollback model. Other aspects of the mid-Cretaceous Bering Strait region differ from areas where trench rollback is well documented, such as the Aegean. Trench retreat is favored by orthogonal subduction of old, cold oceanic lithosphere [*Molnar and Atwater*, 1978; *Carlson and Melia*, 1984]. Magnetic anomalies in the Aleutian Basin are M1 (117 Ma) to M13 (132 Ma) [*Cooper et al.*, 1976]. Therefore this portion of the Kula plate was <80 Myr old when it was trapped by a southward jump of the subduction zone in the late Paleocene. Given that the magnetic anomalies in the Aleutian Basin are orthogonal to the Bering margin and that, as far as we can tell, plate convergence of the Farallon and Kula plates was oblique to the margin during much of the Late Cretaceous [*Engebretson et al.*, 1985], it is unlikely that old oceanic crust was being subducted at the time of formation of the Koolen dome.

5.3. Late Cretaceous–Tertiary Strike-Slip Faulting and Normal Faulting

[53] Northwest striking normal faults and northeast striking right-lateral strike-slip faults cut the Chegitun and

Tanatap units during the last episode of deformation. It is clear that they formed by the time the Tanatap unit had been exhumed into the upper crust. Apatite fission track data from the High-Grade unit and the thermochronologic data of the Koolen dome [*BSGFP*, 1997; *Akinin and Calvert*, 2002] indicate that exhumation of the dome took place in the Late Cretaceous to early Paleocene.

[54] The Hope Basin lies in the offshore area directly northeast of the Chegitun Valley (Figure 1). It is a predominantly extensional basin cut by many west to northwest trending normal faults of similar orientation to those of the Chegitun area (Figure 1). *Tolson* [1987] believed that the basin formed during early Tertiary. However, synextensional deposits of Late Cretaceous age have been identified in seismic profiles of the Russian sector of the Hope Basin [*Gramberg and Pogrebitzkiy*, 1984; *Shipelkevich et al.*, 1998; Y. V. Shipelkevich, personal communication, 1999]; therefore the onset of basin formation may have started earlier.

[55] *Tolson* [1987] attributed the origin of the Hope Basin to transtensional deformation due to right-lateral movement on the Kobuk fault zone, which runs along the south flank of the Brooks Range. *Natal'in* [1999] inferred that the Hope Basin is heterogeneous in nature. Its bigger and older western part was generated by extension in the Late Cretaceous, and this extension continued into the early Tertiary. The Ratkhat and Nynykin faults are viewed as a part of the Chegitun-Lisburne transfer fault that compensated the extension in the western part of the Hope Basin (Figure 1) [*Natal'in*, 1999].

6. Conclusions

[56] Three distinct lithotectonic units bounded by late-stage strike-slip faults are exposed on the NW flank of the Koolen dome. We recognize three main deformational events in these rocks and relate them to Early Cretaceous to Tertiary tectonic evolution of the Bering Strait region. The earliest event was probably due to the collision of the Chukotka–Arctic Alaska block with mainland Asia along the South Anyui suture. It took place before 117–124 Ma and was accompanied by greenschist facies metamorphism and development of S_{1t} fabrics in the Tanatap unit. We also attribute the development of kyanite-bearing assemblages in the High-Grade unit rocks to this event, though we cannot totally dismiss the possibility of a Paleozoic age for these assemblages.

[57] Early Cretaceous contractional structures are overprinted by sillimanite-grade metamorphism and intense ductile deformation related to the evolution of the Koolen dome. In the Chegitun Valley, sillimanite-grade metamorphism was followed by rapid cooling and exhumation between 109 and 104 Ma. This cooling of the flank of the dome took place while peak temperatures prevailed in the core. At shallower structural level, which is represented by the Tanatap unit, early fabrics underwent isoclinal folding and a new cleavage (S_{2t}) was developed. The kinematics of fabrics in the High-Grade unit of the Chegitun Valley indicates that ductile deformation took place by top-to-the south shear. Our structural data from the High-Grade unit combined with data presented by *BSGFP* [1997] suggest that the Koolen dome is an unidirectional core complex formed by south and southeast directed extension and not an anorogenic diapir as has been proposed [*Parfenov and Natal'in*, 1979; *Akinin and Calvert*, 2002].

[58] Candidates for the driving mechanism for mid-Cretaceous N-S extension in the Bering Strait region are (1) postorogenic collapse of overthickened crust facilitated by magmatic weakening of the lower and middle crust [*Natal'in and Toro*, 1998] and (2) rollback of the subduction zone out of the Bering region and toward the paleo-Pacific [*Rubin et al.*, 1995]. We favor the first model and attribute the thickening of the crust both to the collision along the South Anyui–Angayucham suture and to the oroclinal bending of the Paleozoic to early Mesozoic structures in the Bering Strait region. The youngest structures in the Chegitun Valley are NW striking normal faults and NW striking right-lateral strike-slip faults. We believe both sets of structures are kinematically linked and are the continuation of structures found offshore in the western part of the Hope Basin [*Natal'in*, 1999].

[59] **Acknowledgments.** This research was supported by NSF Continental Dynamics Division Award EAR 93-17087 to E.L. Miller and S. Klemperer of Stanford University. We would like to thank the people of Lavrentiya for their hospitality and Slava Akinin for keeping faithful radio contact with us while on the Chegitun River and for picking us up before the Arctic fog swallowed us forever. We also thank Trevor Dumitru for the apatite fission track analysis. The manuscript benefited from insightful comments by E.L. Miller and reviews by Sarah Roeske and Bill McClelland.

References

Akinin, V. V., and A. T. Calvert, Cretaceous mid-crustal metamorphism and exhumation of the Koolen gneiss dome, Chukotka Peninsula, NE Russia, in *Crustal Evolution of the Bering-Chukchi Region of Russia and Alaska and Adjacent Arctic Ocean*, edited by E. L. Miller, A. Grantz, and S. Klemperer, *Spec. Pap. Geol. Soc. Am.*, *360*, 147–166, 2002.

Amato, J. M., and J. E. Wright, Geochronologic investigations of magmatism and metamorphism within the Kigluaik Mountains gneiss dome, Seward Peninsula, Alaska, in *Short Notes on Alaskan Geology 1997*, edited by J. G. Clough and F. Larson, *Prof. Rep. 118*, pp. 1–21, State of Alaska Div. of Geol. and Geophys. Surv., Fairbanks, 1998.

Amato, J. M., J. E. Wright, P. B. Gans, and E. L. Miller, Magmatically induced metamorphism and deformation in the Kigluaik gneiss dome, Seward Peninsula, Alaska, *Tectonics*, *13*, 515–527, 1994.

Armstrong, R. L., R. B. Harakal, B. W. Forbes, B. W. Evans, and S. P. Thurston, Rb/Sr and K/Ar study of metamorphic rocks of the Seward Peninsula and southern Brooks Range, Alaska, in *Blueschists and Eclogites*, vol. 164, edited by B. W. Evans and E. H. Brown, *Mem. Geol. Soc. Am.*, *164*, 185–203, 1986.

Bering Strait Geological Field Party (BSGFP), Koolen metamorphic complex, NE Russia: Implications for the tectonic evolution of the Bering Strait region, *Tectonics*, *16*, 713–729, 1997.

Calvert, A. T., Metamorphism and exhumation of mid-crustal gneiss domes in the Arctic Alaska terrane, Ph.D. thesis, 150 pp., Univ. of Calif., Santa Barbara, 1999.

Carlson, R. L., and P. J. Melia, Subduction hinge migration, *Tectonophysics*, *102*, 399–411, 1984.

Coney, P. J., and T. Harms, Cordilleran metamorphic core complexes: Cenozoic extensional relics of Mesozoic compression, *Geology*, *12*, 550–554, 1984.

Cooper, A. K., D. W. Scholl, and M. S. Marlow, Plate tectonic model for the evolution of the Bering Sea basin, *Geol. Soc. Am. Bull.*, *87*, 1119–1126, 1976.

Dalrymple, G. B., and M. A. Lanphere, $^{40}Ar/^{39}Ar$ age spectra of some undisturbed terrestrial samples, *Geochim. Cosmochim. Acta*, *38*, 715–738, 1974.

Dewey, J. F., Extensional collapse of orogens, *Tectonics*, *7*, 1123–1139, 1988.

Dumitru, T. A., E. L. Miller, J. M. Amato, K. A. Hannula, A. T. Calvert, and P. B. Gans, Cretaceous to Recent extension in the Bering Strait region, Alaska, *Tectonics*, *14*, 549–563, 1995.

Dusel-Bacon, C., W. P. Brosgé, A. B. Till, E. O. Doyle, C. F. Mayfield, H. N. Reiser, and T. P. Miller, Distribution, facies, ages, and proposed tectonic associations of regionally metamorphosed rocks in northern Alaska, *U.S. Geol. Surv. Prof. Pap.*, *P1497-A*, 44 pp., 1989.

Engebretson, D. C., A. Cox, and R. G. Gordon, Relative motions between oceanic and continental plates in the pacific basin, *Spec. Pap. Geol. Soc. Am.*, *206*, 59 pp., 1985.

England, P. S., Constrains on extension of continental lithosphere, *J. Geophys. Res.*, *88*, 1145–1152, 1983.

Fujita, K., and J. T. Newberry, Tectonic evolution of northeastern Siberia and adjacent regions, *Tectonophysics*, *89*, 337–357, 1982.

Galbraith, R. F., On statistical models for fission track counts, *J. Int. Assoc. Math. Geol.*, *13*, 471–478, 1981.

Galbraith, R. F., and G. M. Laslett, Statistical models of mixed fission-track ages, *Nucl. Tracks Radiat. Meas.*, *21*, 459–470, 1993.

Gallagher, K., Genetic algorithms: A powerful new method for modelling fission track data and thermal histories, in *Abstracts of the Eighth International Conference on Geochronology, Cosmochronology, and Isotope Geology*, edited by M. A. Lanphere, G. B. Dalrymple, and B. D. Turrin, *U.S. Geol. Surv. Circ.*, *C1107*, 1994.

Gleadow, A. J. W., I. R. Duddy, P. F. Green, and J. F. Lovering, Confined fission track lengths in apatite: A diagnostic tool for thermal history analysis, *Contrib. Mineral. Petrol.*, *94*, 405–415, 1986.

Gorodinsky, M. E., (Ed.), Geological map of northeastern USSR, map, sheets X-X, scale 1:500,000, Minist. of Geol., Russia, Leningrad, 1980.

Gottschalk, R. R., and L. W. Snee, Tectonothermal evolution of metamorphic rocks in the south-central Brooks Range, Alaska: Constraints from $^{40}Ar/^{39}Ar$ geochronology, in *Architecture of the Central Brooks Range Fold and Thrust Belt, Arctic Alaska*, edited by J. S. Oldow and H. G. Ave Lallemant, *Spec. Pap. Geol. Soc. Am.*, *324*, 225–253, 1998.

Gramberg, I. S., and Y. E. Pogrebitzkiy, *Seas of the Soviet Arctic* (in Russian), vol. 9, in *Geologicheskoe Stroenie SSSR i Zakonomernosti Razmescheniya Poleznykh Iskopaemykh*, edited by E. A. Kozlovsky, Nedra, Leningrad, Russia, 280 pp., 1984.

Grantz, A., S. D. May, and P. E. Hart, Geology of Arctic continental margin of Alaska, in *The Arctic Ocean Region*, edited by A. Grantz, L. Johnson, and J. F. Sweeney, pp. 257–288, Geol. Soc. of Am., Boulder, Colo., 1990.

Green, P. F., A new look at statistics in fission track dating, *Nucl. Tracks*, *5*, 77–86, 1981.

Grove, M., and T. M. Harrison, $^{40}Ar^*$ diffusion in Ferich biotite, *Am. Mineral.*, *81*, 940–951, 1996.

Hacker, B. R., and Q. Wang, Ar/Ar geochronology of ultrahigh-pressure metamorphism in central China, *Tectonics*, *14*, 994–1006, 1995.

Haimila, N. E., C. E. Kirschner, W. W. Nassichuk, G. F. Ulmishek, and R. M. Procter, Sedimentary basins and petroleum resource potential of the Arctic Ocean region, in *The Arctic Ocean Region*, edited by A. Grantz, L. Johnson, and J. F. Sweeney, pp. 503–538, Geol. Soc. of Am., Boulder, Colo., 1990.

Hannula, K. A., E. L. Miller, T. A. Dumitru, J. Lee, and C. M. Rubin, Structural and metamorphic relations in the southwest Seward Peninsula, Alaska: Crustal extension and the unroofing of blueschists, *Geol. Soc. Am Bull.*, *107*, 536–553, 1995.

Harrison, T. M., Diffusion of ^{40}Ar in hornblende, *Contrib. Mineral. Petrol.*, *78*, 324–331, 1981.

Harrison, T. M., I. Duncan, and I. McDougall, Diffusion of ^{40}Ar in biotite: Temperature, pressure and compositional effects, *Geochim. Cosmochim. Acta*, *49*, 2461–2468, 1985.

Hippert, J., and E. Tohver, On the development of zones of reverse shearing in mylonitic rocks, *J. Struct. Geol.*, *21*, 1603–1604, 1999.

Hurford, A. J., and P. F. Green, The zeta age calibration of fission-track dating, *Chem. Geol.*, *41*, 285–317, 1983.

Klemperer, S., et al., Crustal structure of the Bering and Chukchi shelves: Deep seismic reflection profiles across the North American continent between Alaska and Russia, in *Tectonic Evolution of the Bering-Shelf-Chukchi Sea-Arctic Margin and Adjacent Landmasses*, edited by E. L. Miller, A. Grantz, and S. L. Klemperer, *Spec. Pap. Geol. Soc. Am.*, *360*, 1–24, 2002.

Krasny, L. I., and V. K. Putintsev, *Eastern Part of the USSR* (in Russian), vol. 5, in *Geologicheskoe Stroenie SSSR i Zakonomernoski Razmescheniya Poleznykh Iskopaemykh*, edited by E. A. Kozlovsky, Nedra, Leningrad, Russia, 560 pp., 1984.

Lawver, L. A., and C. R. Scotese, A review of tectonic models for the evolution of the Canada basin, in *The Geology of North America*, vol. L, *The Arctic Ocean Region*, edited by A. Grantz, L. Johnson, and J. F. Sweeney, pp. 593–618, Geol. Soc. of Am., Boulder, Colo., 1990.

Lister, G. S., and S. L. Baldwin, Modelling the effect of arbitrary P-T-t histories on argon diffusion in minerals using the MacArgon program for the Apple Macintosh, *Tectonophysics*, *253*, 83–109, 1996.

Lovera, O. M., F. M. Richter, and T. M. Harrison, The $^{40}Ar/^{39}Ar$ thermochronometry for slowly cooled samples having a distribution of diffusion domain sizes, *J. Geophys. Res.*, *94*, 17,917–17,935, 1989.

Miller, E. L., and T. L. Hudson, Mid-Cretaceous extensional fragmentation of a Jurassic-Early Cretaceous compressional orogen, Alaska, *Tectonics*, *10*, 781–796, 1991.

Miller, E. L., A. T. Calvert, and T. A. Little, Strain-collapsed metamorphic isograds in a sillimanite gneiss dome, Seward Peninsula, Alaska, *Geology*, *20*, 487–490, 1992.

Miller, T. P., Pre-Cenozoic plutonic rocks in mainland Alaska, in *The Geology of North America*, vol. G-1, *The Geology of Alaska*, edited by G. Plafker and H. C. Berg, pp. 535–554, Geol. Soc. of Am., Boulder, Colo., 1994.

Molnar, P., and T. Atwater, Interarc spreading and Cordilleran tectonics as alternates related to the age of subducted oceanic lithosphere, *Earth Planet. Sci. Lett.*, *41*, 330–340, 1978.

Moore, T. E., A. Grantz, and S. M. Roeske, Continent-ocean transition in Alaska: Tectonic assembly of eastern Denalia, in *Phanerozoic Evolution of North American Continent-Ocean Transitions*, edited by R. C. Speed, pp. 399–441, Geol. Soc. of Am., Boulder, Colo., 1994a.

Moore, T. E., W. K. Wallace, K. J. Bird, S. M. Karl, C. G. Mull, and J. T. Dillon, Geology of northern Alaska, in *Geology of North America*, vol. G-1, *The Geology of Alaska*, edited by G. Plafker and H. C. Berg, pp. 49–140, Geol. Soc. of Am, Boulder, Colo., 1994b.

Natal'in, B. A., Tectonic nature of the metamorphic complex in Chukotka Peninsula (in Russian), *Geol. Geofiz.*, *6*, 31–38, 1979.

Natal'in, B. A., *Early Mesozoic Folded Belts in the North Part of the Pacific Rim* (in Russian), 135 pp., Nauka, Moscow, 1984.

Natal'in, B. A., Late Cretaceous-Tertiary deformations in the Chukotka Peninsula: Implication for the origin of the Hope Basin and the Herald Thrust Belt (Chukchi Sea), *Geotectonics*, *33*(6), 76–93, 1999.

Natal'in, B. A., and L. M. Parfenov, Symmetry of the Chukotkan and Alaskan faults (in Russian), in *Simmetriya Struktur Geologicheskikh Tel*, vol. 1, pp. 94–95, Nauka, Moscow, 1976.

Natal'in, B. A., and J. Toro, Bering Sea orocline and the formation of the Koolen (Chukotka) and Kigluaik (Seaward Peninsula) metamorphic core complexes, paper presented at 6th Zonenshain Conference on Plate Tectonics and Europrobe Workshop on Uralides, Russ. Acad. of Sci., Moscow, 1998.

Natal'in, B., J. Toro, and J. Amato, The origin of Cretaceous metamorphic core complexes in the Bering Strait area, paper presented at III International Conference on Arctic Margins, Miner. Manage. Serv., Celle, Germany, 1998.

Natal'in, B. A., J. M. Amato, J. Toro, and J. E. Wright, Paleozoic rocks of northern Chukotka Peninsula, Russian Far East: Implications for the tectonics of the Arctic region, *Tectonics*, *18*, 977–1003, 1999.

Nedomolkin, V. F., The state geological map of the USSR, Chegitun (in Russian), map, sheets Q-2-VII, VII, IX, scale 1:200,000, Minist. of Geol., Russia, Leningrad, 1969.

Nedomolkin, V. F., Geology of the Eskimos median massif (in Russian), Avtorferat kandidatskoy dissertatsii, Far East Sci. Cent., Acad. Sci., 16 pp., Vladivostok, Russia, 1977.

Oradovskaya, M. M., and A. M. Obut, Stratigraphy, correlation, and paleogeography of the Ordovician and Silurian strata in Chukotka Peninsula (in Russian), in *Stratigrafiya i Fauna Ordovika i Silura Chukotskogo Poluostrova*, edited by A. M. Obut, pp. 4–42, Nauka, Novosibirsk, Russia, 1977.

Parfenov, L. M., and B. A. Natal'in, Tectonic evolution of north-eastern Asia in the Mesozoic and Cenozoic (in Russian), *Dokl. Acad. Nauk SSSR*, *235*(5), 1132–1135, 1977.

Parfenov, L. M., and B. A. Natal'in, Small sialic blocks, in *Tectonic Subdivision and Structural and Compositional Evolution of Northeastern Asia* (in Russian), pp. 124–133, Nauka, Moscow, 1979.

Parfenov, L. M., and B. A. Natal'in, Mesozoic accretion and collision tectonics of northeastern Asia, in *Tectonostratigraphic Terranes of the Circum-Pacific Region*, vol. 1, edited by D. G. Howell, pp. 363–373, Circum-Pac. Counc. for Energy and Miner. Resour., Houston, Tex., 1985.

Passchier, C. W., and R. A. J. Trouw, *Microtectonics*, Springer-Verlag, New York, 1996.

Patrick, B. E., Synmetamorphic structural evolution of the Seward Peninsula blueschist terrane, *J. Struct. Geol.*, *10*, 555–565, 1988.

Patrick, B. E., and B. W. Evans, Metamorphic evolution of the Seward Peninsula blueschist terrane, *J. Petrol.*, *30*, 531–555, 1989.

Patton, W. W.Jr., and S. E. Box, Tectonic setting of the Yukon-Koyukuk basin and its borderlands, western Alaska, *J. Geophys. Res.*, *94*, 15,807–15,820, 1989.

Patton, W. W., and I. L. Tailleur, Evidence in the Bering Strait region for differential movement between North America and Eurasia, *Geol. Soc. Am. Bull.*, *88*, 1298–1304, 1977.

Plafker, G., and H. C. Berg, Overview of the geology and tectonic evolution of Alaska, in *The Geology of North America*, vol. G-1, *The Geology of Alaska*, edited by G. Plafker and H. C. Berg, pp. 989–1022, Geol. Soc. of Am., Boulder, Colo., 1994.

Rejebian, V. A., A. G. Harris, and J. S. Huebner, Conodont color and textural alteration: An index to regional metamorphism, contact metamorphism, and hydrothermal alteration, *Geol. Soc. Am. Bull.*, *99*, 471–479, 1987.

Reynolds, S. J., and G. S. Lister, Folding of mylonitic zones in Cordilleran metamorphic core complexes: Evidence from near the mylonitic front, *Geology*, *18*, 216–219, 1990.

Rubin, C. M., E. L. Miller, and J. Toro, Deformation of the northern circum-Pacific margin: Variations in tectonic style and plate-tectonic implications, *Geology*, *23*, 897–900, 1995.

Shipelkevich, Y. V., V. V. Kudel'kin, V. F. Kruglyak, and I. V. Shipelkevich, Structure, evolution and hydrocarbon potential of sedimentary basins on the Russian Chukchi shelf, paper presented at III International Conference on Arctic Margins, Miner. Manage. Serv., Celle, Germany, 1998.

Shuldiner, V. I., and V. F. Nedomolkin, Crystalline basement of the Eskimos massif (in Russian), *Sov. Geol.*, *10*, 38–47, 1976.

Sokolov, S. D., G. Y. Bondarenko, O. L. Morozov, V. A. Shekhovtsov, S. P. Glotov, A. V. Ganelin, and I. R. Kravchenko-Berezhnoy, The South Anyui suture, northeast Arctic Russia: Facts and problems, in *Crustal Evolution of the Bering-Chukchi Region of Russia and Alaska and Adjacent Arctic Ocean*, edited by E. L. Miller, A. Grantz, and S. Klemperer, *Spec. Pap. Geol. Soc. Am.*, *360*, 209–225, 2002.

Tolson, R. B., Structure and stratigraphy of the Hope Basin, southern Chukchi Sea, Alaska, in *Geology and Resource Potential of the Continental Margin of Western North America and Adjacent Ocean Basins, Beaufort Sea to Baja California*, edited by D. W. Scholl, A. Grantz, and J. G. Vedder, pp. 59–71, Circum-Pac. Counc. for Energy and Miner. Resour., Houston, Tex., 1987.

Wendlt, I., and C. Carl, The statistical distribution of the mean squared weighted deviation, *Chem. Geol.*, *86*, 275–285, 1991.

Yardley, B. W., *Introduction to Metamorphic Petrology*, Addison-Wesley-Longman, Reading, Mass., 1989.

Zhulanova, I. L., *The Earth Crust of the Northeast of Asia in Precambrian and Phanerozoic Time* (in Russian), *Nauka*, Moscow, 1990.

Zonenshain, L. P., M. I. Kuzmin, and L. M. Natapov (Eds.), *Geology of the USSR: A Plate Tectonic Synthesis*, *Geodyn. Ser.*, vol. 21, AGU, Washington, D. C., 1990.

J. M. Amato, Department of Geological Sciences, New Mexico State University, Las Cruces, NM 88003, USA. (amato@nmsu.edu)

B. Natal'in, Istanbul Technical University, Istanbul, Turkey. (natalin@itu.edu.tr)

J. Toro, Department of Geology and Geography, West Virginia University, Morgantown, WV 26506, USA. (jtoro@wvu.edu)